

Anomalous diffusion and collapse of self-gravitating Langevin particles in D dimensions

Pierre-Henri Chavanis and Clément Sire

May 22, 2019

Laboratoire de Physique Théorique (FRE 2603 du CNRS), Université Paul Sabatier,
118, route de Narbonne, 31062 Toulouse cedex 4, France
E-mail: *chavanis@irsamc.ups-tlse.fr* & *clement.sire@irsamc.ups-tlse.fr*

Abstract

We address the generalized thermodynamics and the collapse of a system of self-gravitating Langevin particles exhibiting anomalous diffusion in a space of dimension D . The equilibrium states correspond to polytropic distributions. The index n of the polytrope is related to the exponent of anomalous diffusion. We consider a high-friction limit and reduce the problem to the study of the nonlinear Smoluchowski-Poisson system. We show that the associated Lyapunov functional is the Tsallis free energy. We discuss in detail the equilibrium phase diagram of self-gravitating polytropes as a function of D and n and determine their stability by using turning points arguments and analytical methods. When no equilibrium state exists, we investigate self-similar solutions describing the collapse. These results can be relevant for astrophysical systems, two-dimensional vortices and for the chemotaxis of bacterial populations. Above all, this model constitutes a prototypical dynamical model of systems with long-range interactions which possesses a rich structure and which can be studied in great detail.

1 Introduction

In preceding papers [1, 2, 3], we have studied a model of self-gravitating Brownian particles enclosed within a box of radius R in a space of dimension D . This model can be considered as a prototypical dynamical model of systems with long-range interactions. For simplicity, we considered the Smoluchowski-Poisson (SP) system which is deduced from the Kramers-Poisson (KP) system in a high friction limit (or for large times). These Fokker-Planck-Poisson equations were first proposed in [1] as a simplified dynamical model of self-gravitating systems. Their relation with thermodynamics (first and second principles) was clearly established in terms of a maximum entropy production principle (MEPP) and their rich properties (self-organized states or collapse) were described qualitatively in this preliminary work. A thorough study of this system of equations was undertaken more recently [2, 3], complemented by rigorous mathematical results (see [4, 5, 6, 7, 8] and references therein).

The Smoluchowski equation is a particular Fokker-Planck equation involving a diffusion and a drift [9]. In our model, the drift is directed toward the region of high densities due to the gravitational force which is generated by the particles themselves. This retroaction leads to a situation of collapse when attraction prevails over diffusion [2, 3]. The SP system

also provides a simplified model for the chemotactic aggregation of bacterial populations [10] and for the clustering of point vortices in two-dimensional hydrodynamics [11, 12, 13]. It can be shown that the SP system increases continuously a free energy constructed with the Boltzmann entropy [1, 2]. Accordingly, the stationary solutions of the SP system are given by the Boltzmann distribution which maximizes Boltzmann's free energy at fixed mass. The equilibrium state is then determined by solving the Boltzmann-Poisson (or Emden) equation [14]. However, depending on the value of the control parameter (energy E or temperature T), an equilibrium solution does not always exist and the system can undergo a catastrophic collapse. We determined analytically and numerically self-similar solutions leading to a finite time singularity [2, 3]. In the canonical ensemble (fixed T), the evolution continues after the collapse until a Dirac peak is formed [3, 15].

In this paper, we propose to extend our study to a generalized class of Smoluchowski equations [16]. They can be obtained from the familiar Smoluchowski equation by assuming that the diffusion coefficient depends on the density while the drift coefficient is constant (or the opposite). For simplicity, we shall assume that the diffusion coefficient is a power law of the density. In the absence of drift, this would lead to anomalous diffusion. If we take into account a drift term and a self-attraction, we have to solve the nonlinear Smoluchowski-Poisson (NSP) system. It can be shown [16, 17] that the NSP system increases continuously a free energy associated with Tsallis entropy [18]. Accordingly, the stationary solutions of the NSP system are given by a polytropic distribution which maximizes Tsallis' free energy at fixed mass. The equilibrium state is then determined by solving the Lane-Emden equation [14]. Depending on the value of the control parameter and on the index n of the polytrope, three situations can occur: (i) the NSP system can relax toward an incomplete polytrope maintained by the walls of the confining box (ii) the NSP system can relax toward a complete polytrope of radius $R_* < R$, unaffected by the box (iii) the NSP system can undergo a catastrophic collapse leading to a finite time singularity.

In Secs. 2.1-2.5, we determine the complete equilibrium phase diagram of polytropic spheres for different values of n and D . The polytropic index n can have different physical interpretations. In the context of anomalous diffusion, it is related to the exponent of anomalous diffusion [19]. In the context of stellar structure, it is determined by physical processes (convection, radiation, quantum degeneracy...) [14]. In the context of collisionless self-gravitating systems, it can characterize the degree of mixing in case of incomplete relaxation [20]. On the other hand, non-integer values of D can arise when phase space has a fractal structure. This can be the case in astrophysics and in cosmology, and for other systems of physical interest. It is also possible that systems display physical parameters that *formally* play the role of a non-integer dimension D . We shall exhibit particular dimensions $D = 2$, $D = 4$, $D = 2(1 + \sqrt{2})$ and $D = 10$ which play a special role in our problem. The dimension $D = 2$ is *critical* because the results established for $D > 2$ cannot be directly extended to $D = 2$ [3]. On the other hand, the nature of the caloric curve changes for $D = 4$ and $D = 10$. In Sec. 2.6, we study the stability of polytropic spheres by determining whether they are maxima or minima (or saddle points) of a thermodynamical potential (Tsallis entropy in the microcanonical ensemble and Tsallis free energy in the canonical ensemble). This extends the study performed by Taruya & Sakagami [21, 22] and Chavanis [23, 20] in $D = 3$. In Sec. 3, we show that the NSP system admits self-similar solutions describing a collapse and leading to a finite time singularity. The density decreases at large distances as $\rho \sim r^{-\alpha}$. In the generalized canonical situation, the scaling exponent is $\alpha_n = 2n/(n-1)$ where n is the polytropic index. In the generalized microcanonical situation, the scaling equation has solutions for $\alpha_n \leq \alpha \leq \alpha_{\max}(n, D)$ where $\alpha_{\max}(n, D)$ is a non-trivial exponent. The value of α effectively selected by the system is determined by the dynamics. In Sec. 4, we perform direct numerical simulations of the SP and NSP systems with

high accuracy. We confirm the scaling regime and discuss the value of the scaling exponent. In the microcanonical ensemble, we give numerical evidence that $\alpha = \alpha_n$ so that the temperature is finite at the collapse time (this observation has been made independently by [8]). However, the convergence to this value is so slow that the evolution displays a pseudo-scaling regime with $\alpha_n \leq \alpha \leq \alpha_{\max}$ for the densities achieved. We explain the physical reason for this behavior and we conjecture that $\alpha \simeq \alpha_{\max}$ will be reached in more realistic models (with non-uniform temperature). This paper closely follows the presentation of our companion paper for isothermal spheres [3]. These two papers complete the classical monograph of Chandrasekhar on self-gravitating isothermal and polytropic spheres [14].

2 Equilibrium structure of polytropic spheres in dimension D

2.1 Generalized thermodynamics

Consider a system of N particles with mass m interacting via Newtonian gravity in a space of dimension D . The particles are enclosed within a box of radius R . Let $f(\mathbf{r}, \mathbf{v}, t)$ denote the distribution function of the system, i.e. $f(\mathbf{r}, \mathbf{v}, t)d^D\mathbf{r}d^D\mathbf{v}$ gives the mass of particles whose position and velocity are in the cell $(\mathbf{r}, \mathbf{v}; \mathbf{r} + d^D\mathbf{r}, \mathbf{v} + d^D\mathbf{v})$ at time t . The integral of f over the velocity determines the spatial density

$$(1) \quad \rho = \int f d^D\mathbf{v}.$$

The total mass of the configuration is

$$(2) \quad M = \int \rho d^D\mathbf{r}.$$

In the mean-field approximation, the total energy of the system can be expressed as

$$(3) \quad E = \frac{1}{2} \int f v^2 d^D\mathbf{r}d^D\mathbf{v} + \frac{1}{2} \int \rho \Phi d^D\mathbf{r} = K + W,$$

where K is the kinetic energy and W the potential energy. The gravitational potential Φ is related to the density by the Newton-Poisson equation

$$(4) \quad \Delta\Phi = S_D G \rho,$$

where S_D is the surface of a unit sphere in a D -dimensional space and G is the constant of gravity.

We shall first assume that the system is isolated so that it conserves mass and energy. This characterizes a microcanonical situation. We assume furthermore that the equilibrium state maximizes the Tsallis entropy

$$(5) \quad S_q = -\frac{1}{q-1} \int (f^q - f) d^D\mathbf{r}d^D\mathbf{v},$$

at fixed mass M and energy E , where q is a real number. For $q \rightarrow 1$, Eq. (5) reduces to the ordinary Boltzmann entropy. We shall also consider a canonical situation in which the equilibrium state maximizes the Tsallis free energy

$$(6) \quad J_q = S_q - \frac{1}{T} E,$$

at fixed mass M and (generalized) temperature T . As discussed in Refs. [16] and [20] these variational principles can have different physical applications. They arise for example in the context of anomalous diffusion and nonlinear Fokker-Planck equations. The relation with the nonlinear Smoluchowski-Poisson system will be made explicitly in Sec. 3. They also determine the nonlinear dynamical stability of stellar polytropes and gaseous polytropes with respect to the Vlasov and Navier-Stokes equations (see [20]) and the dynamical stability of 2D vortices with respect to the 2D Euler equation (see [16]). For the moment, we shall consider these variational problems on general grounds without direct reference to a precise context. We stress that these variational problems can arise in problems of physics (or biology, economy,...) which have no direct relation to thermodynamics. However, since they are *similar* to the ordinary variational problems arising in classical thermodynamics (with the Boltzmann entropy) it is relevant to use a thermodynamical language and develop a *thermodynamical analogy* [16] [20]. We shall encounter some *thermodynamical anomalies* in the discussion which attest of the greater generality of our problem.

The critical points of entropy at fixed mass and energy satisfy the condition

$$(7) \quad \delta S_q - \beta \delta E - \lambda \delta M = 0,$$

where $\beta = 1/T$ and λ are Lagrange multipliers (T is the temperature). The variational principle (7) leads to the polytropic distribution function

$$(8) \quad f = A \left[\alpha - \Phi - \frac{v^2}{2} \right]^{\frac{1}{q-1}},$$

$$(9) \quad A = \left[\frac{(q-1)\beta}{q} \right]^{\frac{1}{q-1}}, \quad \alpha = \frac{1 - (q-1)\lambda}{(q-1)\beta}.$$

Of course, the same results are obtained by extremizing Tsallis free energy (6) at fixed mass. Equation (8) is valid for $v^2/2 \leq \alpha - \Phi$. If $v^2/2 \geq \alpha - \Phi$, we set $f = 0$. We define the polytropic index n by the relation

$$(10) \quad n = \frac{D}{2} + \frac{1}{q-1}.$$

We shall discuss any value of $n \geq 0$. We note that $f'(\epsilon) < 0$ for $n > D/2$ and $f'(\epsilon) > 0$ for $n < D/2$, where $\epsilon = \frac{v^2}{2} + \Phi$ is the stellar energy. The case $n < D/2$ is not physical for stellar polytropes [24] but it *is* physical for gaseous polytropes [14], so it will be considered in our general study. We note that $f(\epsilon)$ is a step function for $n_{3/2} = D/2$ (obtained for $q \rightarrow \pm\infty$). This corresponds to the self-gravitating Fermi gas at zero temperature. Indeed, classical white dwarf stars are equivalent to polytropes with index $n = 3/2$ in $D = 3$ [14]. When $(q-1)/q < 0$, Eqs. (8)-(9) remain valid with $\beta < 0$. Since β is a formal Lagrange multiplier, there is no paradox in considering *negative* temperature states. However, it can be convenient to define a temperature T_* by

$$(11) \quad (n+1)T_* = \frac{q}{(q-1)}T.$$

This temperature is always positive and coincides with the usual temperature for $n \rightarrow +\infty$ (or $q \rightarrow 1$). We can also define specific heats by $C = dE/dT$ and $C_* = dE/dT_*$. We note that $C < 0$ with $T < 0$ is equivalent to $C_* > 0$. We must keep in mind these remarks when discussing the caloric curves in Sec. 2.5.

Using Eq. (8), the spatial density $\rho = \int f d^D \mathbf{v}$ and the pressure $p = \frac{1}{D} \int f v^2 d^D \mathbf{v}$ can be expressed as

$$(12) \quad \rho = 2^{D/2-1} A S_D (\alpha - \Phi)^n B(D/2, n+1 - D/2),$$

$$(13) \quad p = \frac{1}{n+1} 2^{D/2-1} A S_D (\alpha - \Phi)^{n+1} B(D/2, n+1 - D/2),$$

with $B(a, b)$ being the beta-function. In obtaining Eq. (13), we have used the identity $B(m+1, n) = mB(m, n)/(m+n)$. The integrability condition $\int f d^D \mathbf{v} < \infty$ requires that $n > D/2 - 1$. Eliminating the gravitational potential between these two relations, we recover the well-known fact that stellar polytropes satisfy the equation of state

$$(14) \quad p = K \rho^\gamma, \quad \gamma = 1 + \frac{1}{n},$$

like gaseous polytropes. In the present context, the polytropic constant is given by

$$(15) \quad K = \frac{1}{(n+1)} \left\{ 2^{D/2-1} S_D A B(D/2, n+1 - D/2) \right\}^{-1/n}.$$

Using Eqs. (9) and (12), the distribution function (8) can be written as a function of the density as

$$(16) \quad f = \frac{1}{Z} \left[\rho^{1/n} - \frac{v^2/2}{(n+1)K} \right]^{n-D/2},$$

with

$$(17) \quad Z = 2^{D/2-1} S_D B(D/2, n+1 - D/2) [K(n+1)]^{D/2}.$$

It is now possible to express the energy (3) and the entropy (5) in terms of $\rho(\mathbf{r})$ and T . Using Eq. (8) and the foregoing relations, it is easy to show that

$$(18) \quad E = \frac{D}{2} \int p d^D \mathbf{r} + \frac{1}{2} \int \rho \Phi d^D \mathbf{r},$$

$$(19) \quad S_q = - \left(n - \frac{D}{2} \right) \left(\beta \int p d^D \mathbf{r} - M \right).$$

In arriving at Eq. (19), we have used the identity $B(m, n+1) = nB(m, n)/(m+n)$. Proceeding carefully, we can check that for $q \rightarrow 1$, Eq. (19) reduces to the expression of the Boltzmann entropy in configuration space (see Eq. (9) of [3]).

The equilibrium state is obtained by substituting Eq. (8) in the Poisson equation (4) using Eq. (1). This yields a self-consistent mean-field equation for the gravitational potential Φ . An equivalent equation can be obtained from the condition of hydrostatic equilibrium

$$(20) \quad \nabla p = -\rho \nabla \Phi,$$

and the equation of state (14) (the equivalence between these two approaches is shown in [16]). Using the Gauss theorem

$$(21) \quad \frac{d\Phi}{dr} = \frac{GM(r)}{r^{D-1}},$$

where $M(r) \equiv \int_0^r \rho S_D r'^{D-1} dr'$ is the mass within the sphere of radius r , we can rewrite Eq. (20) in the form

$$(22) \quad \frac{1}{r^{D-1}} \frac{d}{dr} \left(\frac{r^{D-1}}{\rho} \frac{dp}{dr} \right) = -S_D G \rho,$$

which is the fundamental equation of hydrostatic equilibrium in D -dimensions. For the polytropic equation of state (14), we have

$$(23) \quad K(n+1) \frac{1}{r^{D-1}} \frac{d}{dr} \left(r^{D-1} \frac{d\rho^{1/n}}{dr} \right) = -S_D G \rho.$$

The case of isothermal spheres with an equation of state $p = \rho T$ is recovered in the limit $n \rightarrow +\infty$.

2.2 The D -dimensional Lane-Emden equation

To determine the structure of polytropic spheres, we set

$$(24) \quad \rho = \rho_0 \theta^n, \quad \xi = \left[\frac{S_D G \rho_0^{1-1/n}}{K(n+1)} \right]^{1/2} r,$$

where ρ_0 is the central density. Then, Eq. (23) can be put in the form

$$(25) \quad \frac{1}{\xi^{D-1}} \frac{d}{d\xi} \left(\xi^{D-1} \frac{d\theta}{d\xi} \right) = -\theta^n,$$

which is the D -dimensional generalization of the Lane-Emden equation [14]. For $D > 2$ and

$$(26) \quad n > \frac{D}{D-2} \equiv n_3,$$

Eq. (25) has a simple explicit solution, the singular polytropic sphere

$$(27) \quad \theta_s = \left\{ \frac{2[(D-2)n - D]}{(n-1)^2} \right\}^{\frac{1}{n-1}} \xi^{-\frac{2}{n-1}}.$$

The regular solutions of Eq. (25) satisfying the boundary conditions

$$(28) \quad \theta = 1, \quad \theta' = 0 \quad \text{at} \quad \xi = 0,$$

must be computed numerically. For $\xi \rightarrow 0$, we can expand the solutions in Taylor series and we find that

$$(29) \quad \theta = 1 - \frac{1}{2D} \xi^2 + \frac{n}{8D(D+2)} \xi^4 + \dots$$

To obtain the asymptotic behavior of the solutions for $\xi \rightarrow +\infty$, we note that the transformation $t = \ln \xi$, $\theta = \xi^{-2/(n-1)} z$ changes Eq. (25) in

$$(30) \quad \frac{d^2 z}{dt^2} + \frac{(D-2)n - (D+2)}{n-1} \frac{dz}{dt} = -z^n - \frac{2[D + (2-D)n]}{(n-1)^2} z.$$

For $D \leq 2$ or for $D > 2$ and

$$(31) \quad n < \frac{D+2}{D-2} \equiv n_5,$$

the density falls off to zero at a finite radius R_* . This defines a *complete polytrope* of radius R_* . If we denote by ξ_1 the value of the normalized distance at which $\theta = 0$, then, for $\xi \rightarrow \xi_1$, we have

$$(32) \quad \theta = -\xi_1 \theta'_1 \left[\frac{\xi_1 - \xi}{\xi_1} + \frac{D-1}{2} \left(\frac{\xi_1 - \xi}{\xi_1} \right)^2 + \frac{D(D-1)}{6} \left(\frac{\xi_1 - \xi}{\xi_1} \right)^3 + \dots \right].$$

On the other hand, for $D > 2$ and $n > n_5$, Eq. (30) corresponds to the damped motion of a fictitious particle in a potential

$$(33) \quad V(z) = \frac{D + (2-D)n}{(n-1)^2} z^2 + \frac{1}{n+1} z^{n+1},$$

where z plays the role of position and t the role of time. For $t \rightarrow +\infty$, the particle will come at rest at the bottom of the well at position $z_0 = \{2[(D-2)n - D]/(n-1)^2\}^{\frac{1}{n-1}}$. Returning to original variables, we find that

$$(34) \quad \theta \rightarrow \left\{ \frac{2[(D-2)n - D]}{(n-1)^2} \right\}^{\frac{1}{n-1}} \xi^{-\frac{2}{n-1}} = \theta_s, \quad \text{for} \quad \xi \rightarrow +\infty.$$

Therefore, the regular solutions of the Lane-Emden equation (25) behave like the singular solution for $\xi \rightarrow +\infty$. To determine the next order correction, we set $z = z_0 + z'$ with $z' \ll 1$. Keeping only terms that are linear in z' , Eq. (30) becomes

$$(35) \quad \frac{d^2 z'}{dt^2} + \frac{(D-2)n - (D+2)}{n-1} \frac{dz'}{dt} + \frac{2[(D-2)n - D]}{n-1} z' = 0.$$

The discriminant associated with this equation is

$$(36) \quad \Delta(n) = \frac{-(D-2)(10-D)n^2 - 2(D^2 - 8D + 4)n + (D-2)^2}{(n-1)^2}.$$

For $n \rightarrow +\infty$, $\Delta(n) \sim -(D-2)(10-D)$. Furthermore, $\Delta(n) = 0$ for

$$(37) \quad n_{\pm} = \frac{-D^2 + 8D - 4 \pm 8\sqrt{D-1}}{(D-2)(10-D)}.$$

For $2 < D < 10$, it is straightforward to check that $n_- < n_+ < n_5$. Therefore, for $n > n_5$, Δ has the sign of $-(D-2)(10-D)$ which is negative. Thus

$$(38) \quad \theta = \theta_s \left\{ 1 + \frac{C}{\xi^{b/2}} \cos \left(\frac{\sqrt{-\Delta}}{2} \ln \xi + \delta \right) \right\}, \quad (\xi \rightarrow +\infty),$$

where $b = [(D-2)n - (D+2)]/(n-1)$. The density profile (38) intersects the singular solution (27) infinitely often at points that asymptotically increase geometrically in the ratio $1 : \exp\{2\pi/\sqrt{-\Delta}\}$ (see, e.g., Fig. 1 of Ref. [23] for $D = 3$). For $D > 10$, we have $n_+ < n_5 < n_-$. Therefore, if $n_5 < n < n_-$, Δ has the sign of $(D-2)(10-D)$ which is negative and the

asymptotic behavior of the solutions is still given by Eq. (38). However, for $n > n_-$, $\Delta(n)$ is positive and therefore

$$(39) \quad \theta = \theta_s \left\{ 1 + \frac{1}{\xi^{b/2}} \left(A \xi^{\frac{\sqrt{\Delta}}{2}} + B \xi^{-\frac{\sqrt{\Delta}}{2}} \right) \right\}, \quad (\xi \rightarrow +\infty).$$

Finally, for $n = n_-$, $\Delta = 0$ and we have

$$(40) \quad \theta = \theta_s \left\{ 1 + \frac{1}{\xi^{b/2}} (A \ln \xi + B) \right\}, \quad (\xi \rightarrow +\infty).$$

For $D = 10$, $n_- \rightarrow +\infty$ so that the asymptotic behavior of θ is given by Eq. (38) for $n < +\infty$. Since $\theta^n \sim \xi^{-2n/(n-1)}$ at large distances, the configurations described previously have an “infinite mass” which is clearly unphysical. In the following, we shall confine these configurations to a “box” of radius R as for isothermal spheres [3]. Such configurations will be called *incomplete polytropes*. We note that the self-gravitating Fermi gas at zero temperature forms a complete polytrope only if $n_{3/2} < n_5$, i.e. $D < 2(1 + \sqrt{2}) \simeq 4.83$.

The Lane-Emden equation can be solved analytically for some particular values of the polytropic index. For $n = 0$, which corresponds to a body with constant density, we have

$$(41) \quad \theta = 1 - \frac{1}{2D} \xi^2, \quad \xi_1 = \sqrt{2D}.$$

For $n = 1$, Eq. (25) reduces to the D -dimensional Helmholtz equation. For $D = 1$,

$$(42) \quad \theta = \cos \xi, \quad \xi_1 = \frac{\pi}{2}.$$

For $D = 2$,

$$(43) \quad \theta = J_0(\xi), \quad \xi_1 = 2.40482\dots$$

Finally, for $D = 3$, performing the change of variables $\theta = \chi/\xi$, we get

$$(44) \quad \theta = \frac{\sin \xi}{\xi}, \quad \xi_1 = \pi.$$

The Lane-Emden equation can also be solved analytically in any dimension of space $D \geq 2$ for the particular index value n_5 . The solution is

$$(45) \quad \theta_5 = \frac{1}{\left(1 + \frac{\xi^2}{D(D-2)}\right)^{\frac{D-2}{2}}},$$

as can be checked by a direct substitution in Eq. (25). For $D = 3$, we recover the Schuster solution [14]. We note that $\theta_5 \sim \xi^{2-D}$ for $\xi \rightarrow +\infty$ implying a finite mass. This contrasts with the asymptotic behavior (34) of the solutions of the Lane-Emden equation with index $n > n_5$. For $D = 2$, $n_5 \rightarrow +\infty$ and we are lead back to the isothermal case where an analytical solution is also known [3].

Finally, for $D = 1$, the Lane-Emden equation reduces to the form

$$(46) \quad \frac{d^2\theta}{d\xi^2} = -\theta^n.$$

This equation corresponds to the motion of a fictitious particle in a potential $V(\theta) = \theta^{n+1}/(n+1)$, where θ plays the role of position and ξ the role of time. The solution can be written in integral form as

$$(47) \quad \int_{\theta}^1 \frac{dx}{(1-x^{n+1})^{1/2}} = \left(\frac{2}{n+1}\right)^{1/2} \xi.$$

Except for $n = 0$ and $n = 1$, it seems not possible to obtain $\theta(\xi)$ in a closed form. However, the zero ξ_1 of θ is explicitly given by

$$(48) \quad \xi_1 = \left(\frac{n+1}{2}\right)^{1/2} \sqrt{\pi} \frac{\Gamma(\frac{2+n}{1+n})}{\Gamma(\frac{3+n}{2(1+n)})}$$

Therefore, $\xi_1 \sim \sqrt{n/2}$ for $n \rightarrow +\infty$.

2.3 The Milne variables

As is well-known [14], polytropic spheres satisfy a homology theorem: if $\theta(\xi)$ is a solution of the Lane-Emden equation, then $A^{2/(n-1)}\theta(A\xi)$ is also a solution, with A an arbitrary constant. This means that the profile of a polytropic configuration of index n is always the same (characterized intrinsically by the function θ), provided that the central density and the typical radius are rescaled appropriately. Because of this homology theorem, the second order differential equation (25) can be reduced to a *first order* differential equation for the Milne variables

$$(49) \quad u = -\frac{\xi\theta^n}{\theta'} \quad \text{and} \quad v = -\frac{\xi\theta'}{\theta}.$$

Taking the logarithmic derivative of u and v with respect to ξ and using Eq. (25), we get

$$(50) \quad \frac{1}{u} \frac{du}{d\xi} = \frac{1}{\xi} (D - nv - u),$$

$$(51) \quad \frac{1}{v} \frac{dv}{d\xi} = \frac{1}{\xi} (2 - D + u + v).$$

Taking the ratio of the foregoing equations, we obtain

$$(52) \quad \frac{u}{v} \frac{dv}{du} = -\frac{u + v - D + 2}{u + nv - D}.$$

The solution curve in the (u, v) plane is plotted in Figs. 1-4 for different values of D and n . The (u, v) curve is parameterized by ξ . It starts, at $\xi = 0$, from the point $(u, v) = (D, 0)$ with a slope $(dv/du)_0 = -(D+2)/nD$. The points of horizontal tangent are determined by $u + v - D + 2 = 0$ and the points of vertical tangent by $u + nv - D = 0$. These two lines intersect at

$$(53) \quad u_s = \frac{(D-2)n - D}{n-1}, \quad v_s = \frac{2}{n-1},$$

which corresponds to the singular solution (27).

The Milne variables can be expressed in terms of ξ explicitly for particular values of the polytropic index. For $n = 0$, using Eq. (41), we have

$$(54) \quad u = D, \quad v = \frac{2\xi^2}{2D - \xi^2}.$$

For $n = n_5$, using Eq. (45), we have

$$(55) \quad u = \frac{D}{1 + \frac{\xi^2}{D(D-2)}}, \quad v = \frac{1}{D} \frac{\xi^2}{1 + \frac{\xi^2}{D(D-2)}}.$$

Eliminating ξ between these two relations, we get

$$(56) \quad \frac{D}{D-2}v + u = D.$$

More generally, using the asymptotic behavior of $\theta(\xi)$ determined in Sec. 2.2, we can deduce the form of the solution curve in the (u, v) plane. For $(2 < D < 10, n > n_5)$ and for $(D > 10, n_5 < n < n_-)$, the solution curve spirals indefinitely around the limit point (u_s, v_s) . For $(D > 10, n > n_-)$, the curve reaches the point (u_s, v_s) without spiraling. For $D = 10$, $n_- \rightarrow +\infty$ and $n_5 = 3/2$. For $D < 2$ and for $(D > 2, n < n_5)$, the (u, v) curve is monotonic and tends to $(u, v) = (0, +\infty)$ as $\xi \rightarrow \xi_1$. More precisely, using Eq. (32), we have for $n < +\infty$

$$(57) \quad uv^n \sim \omega_n^{n-1}, \quad \omega_n = -\xi_1^{\frac{n+1}{n-1}} \theta'_1 \quad (\xi \rightarrow \xi_1).$$

For $n \rightarrow +\infty$, $\xi_1 \rightarrow +\infty$ and we are lead to our previous study [3]. For $D = 2$, $n_5 \rightarrow +\infty$.

For $n \rightarrow +\infty$, it is easy to check that the Lane-Emden function θ (for polytropes) is related to the Emden function ψ (for isothermal spheres) by the equivalent

$$(58) \quad \theta^n \sim \frac{1}{n} e^{-\psi}.$$

This suggests to introduce the variables $U = u$ and $V = (n+1)v$ instead of (49). For $n \rightarrow +\infty$, U and V tend to the Milne variables u, v defined in the case of isothermal spheres (see [3]). We could have introduced these variables since the beginning but we prefer to respect the notations used by Chandrasekhar in his classical monograph [14].

2.4 The thermodynamical parameters

For a polytrope confined within a box of radius R , the solution of Eq. (25) is terminated by the box at the normalized radius (see Eq. (24))

$$(59) \quad \alpha = \left[\frac{S_D G \rho_0^{1-1/n}}{K(n+1)} \right]^{1/2} R.$$

We shall now relate the parameter α to the polytropic constant K (or generalized temperature T) and to the energy E . Starting from the relation

$$(60) \quad M = \int_0^R \rho S_D r^{D-1} dr = S_D \rho_0 \left[\frac{K(1+n)}{S_D G \rho_0^{1-1/n}} \right]^{D/2} \int_0^\alpha \theta^n \xi^{D-1} d\xi,$$

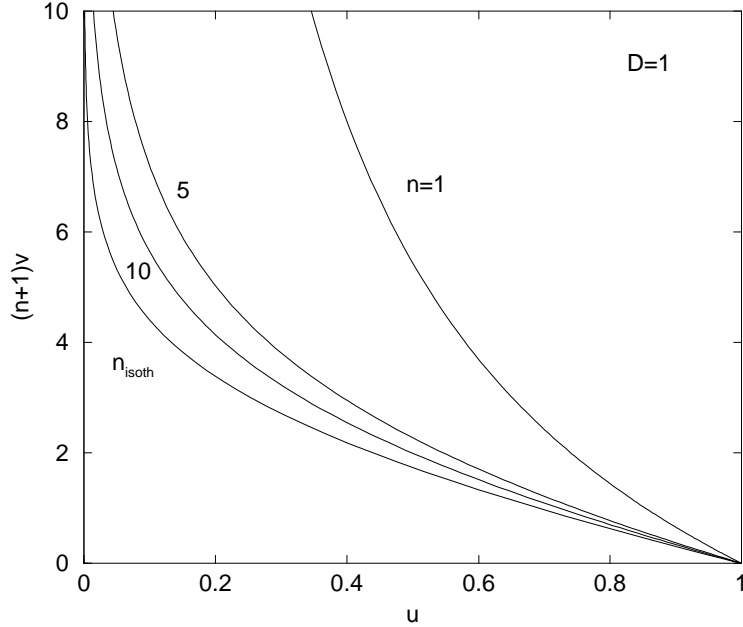


Figure 1: Phase portrait of the Lane-Emden equation in the (u, v) plane for $D < 2$ (specifically $D = 1$). The value of the polytropic index is indicated on each curve. For $n \rightarrow +\infty$, denoted n_{isoth} , we recover the phase portrait of isothermal spheres.

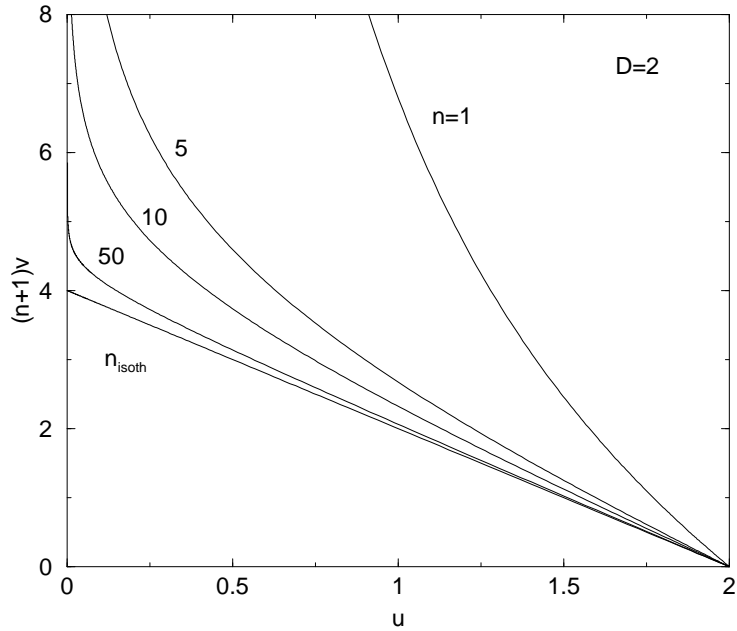


Figure 2: Phase portrait of the Lane-Emden equation in the (u, v) plane for $D = 2$. At this dimension $n_5 \rightarrow +\infty$, so that the $2D$ -Schuster solution (45) becomes equivalent to the $2D$ -isothermal solution [3]. In the (u, v) plane this corresponds to a straight line.

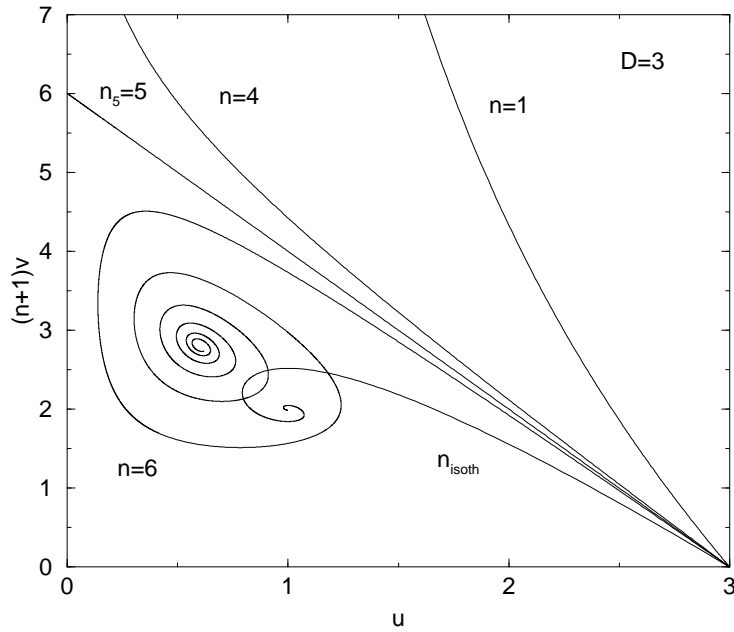


Figure 3: Phase portrait of the Lane-Emden equation in the (u, v) plane for $2 < D < 10$ (specifically $D = 3$).

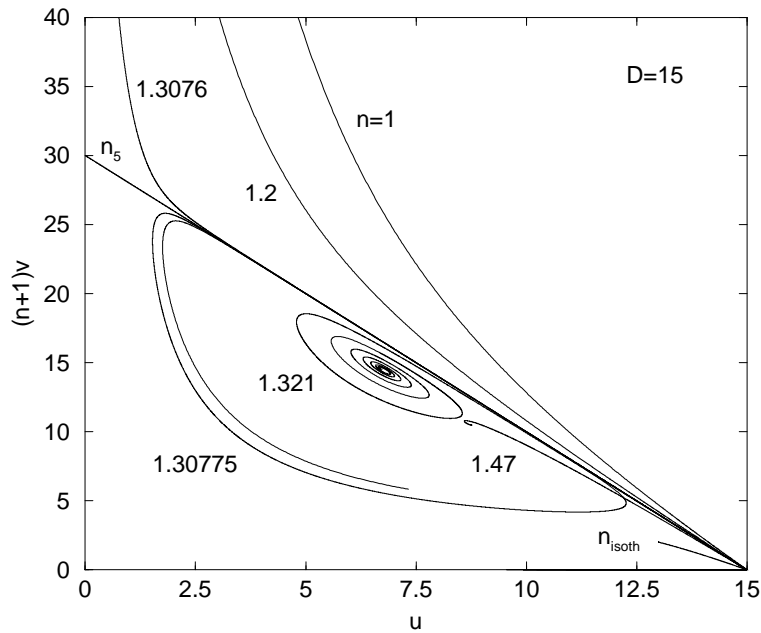


Figure 4: Phase portrait of the Lane-Emden equation in the (u, v) plane for $D > 10$ (specifically $D = 15$). For $D = 10$, $n_- \rightarrow +\infty$. Therefore, for $n > n_5 = 3/2$, the phase portrait is always a spiral except for the index $n = +\infty$ for which the spiral is reduced to a point.

and using the Lane-Emden equation (25), we get

$$(61) \quad M = -S_D \rho_0 \left[\frac{K(1+n)}{S_D G \rho_0^{1-1/n}} \right]^{D/2} \alpha^{D-1} \theta'(\alpha).$$

Expressing the central density in terms of α , using Eq. (59), we obtain after some rearrangements

$$(62) \quad M = -S_D \left[\frac{K(1+n)}{S_D G} \right]^{\frac{n}{n-1}} R^{\frac{(D-2)n-D}{n-1}} \alpha^{\frac{n+1}{n-1}} \theta'(\alpha).$$

For a complete polytrope, the foregoing equation determines the mass-radius relation. Indeed, writing $\alpha = \xi_1$, we get

$$(63) \quad M^{\frac{n-1}{n}} R_*^{\frac{(D-2)(n_3-n)}{n}} = \frac{K(1+n)}{G S_D^{1/n}} \omega_n^{\frac{n-1}{n}},$$

where R_* is the radius of the polytrope and ω_n is defined by Eq. (57). For $n = n_3$, the mass is independent on the radius. This mathematical property is related to the limiting mass of Chandrasekhar for relativistic white dwarf stars [14]. For incomplete polytropes, the parameter

$$(64) \quad \eta \equiv \frac{M}{S_D} \left[\frac{S_D G}{K(1+n)} \right]^{\frac{n}{n-1}} \frac{1}{R^{\frac{(D-2)n-D}{n-1}}},$$

can be considered as a normalized inverse temperature [23]. Indeed, for a given mass M and box radius R , it simply depends on the polytropic constant K which is itself related to β via Eqs. (15) and (9). In addition, for $n \rightarrow +\infty$, the parameter η reduces to the corresponding one for isothermal spheres ($\eta \sim \eta_\infty/n$, $\eta_\infty = \frac{\beta G M m}{R^{D-2}}$, $\beta = 1/kT$) [3]. In terms of this parameter, Eq. (62) can be rewritten

$$(65) \quad \eta = -\alpha^{\frac{n+1}{n-1}} \theta'(\alpha).$$

This relation can be expressed in terms of the values of the Milne variables at the normalized box radius. Writing $u_0 = u(\alpha)$ and $v_0 = v(\alpha)$, we get

$$(66) \quad \eta = (u_0 v_0^n)^{\frac{1}{n-1}}.$$

For a given box radius R and a given polytropic constant K (or generalized temperature T), this equation determines the relation between the mass M and the central density ρ_0 (through the parameter α). For $D \leq 2$ and for ($D > 2$, $n < n_5$), the normalized box radius α is necessarily restricted by the inequality $\alpha \leq \xi_1$. For the limiting value $\alpha = \xi_1$, corresponding to a complete polytrope with radius $R_* = R$, we have

$$(67) \quad \eta(\xi_1) = \omega_n.$$

Alternatively, for $\eta > \omega_n$, $R_* < R$. For the index $n = n_5$, we have explicitly

$$(68) \quad \eta = \frac{\alpha^{\frac{D+2}{2}}}{D \left(1 + \frac{\alpha^2}{D(D-2)} \right)^{D/2}}.$$

For $\alpha \rightarrow +\infty$, we observe that $\eta \sim (3/\alpha)^{1/2}$ for $D = 3$.

The computation of the energy is a little more intricate. We first recall the expression of the Virial theorem in dimension $D \neq 2$ (see Appendix A):

$$(69) \quad 2K + (D - 2)W = DV_D R^D p(R),$$

where $V_D = S_D/D$ is the volume of a hypersphere with unit radius (the kinetic energy K and the potential energy W are defined in Eq. (18)). For $D = 2$, the expression of the Virial theorem is (see Appendix A):

$$(70) \quad 2K - \frac{GM^2}{2} = 2\pi R^2 p(R).$$

The potential energy of a polytrope can be calculated as follows. Combining the condition of hydrostatic equilibrium (20) with the equation of state (14), we get

$$(71) \quad (n + 1) \frac{d}{dr} \left(\frac{p}{\rho} \right) = - \frac{d\Phi}{dr}.$$

This equation integrates to give

$$(72) \quad \Phi = -(n + 1) \left(\frac{p}{\rho} - \frac{p(R)}{\rho(R)} \right) + \Phi(R).$$

Inserting this relation in the integral (3) defining the potential energy W and recalling that the kinetic energy can be written $K = (D/2) \int p d^D \mathbf{r}$, we obtain

$$(73) \quad W = -\frac{1}{D}(n + 1)K + \frac{1}{2}(n + 1) \frac{p(R)}{\rho(R)} M + \frac{1}{2} M \Phi(R).$$

For $D \neq 2$, $\Phi(R) = -GM/[(D - 2)R^{D-2}]$ and for $D = 2$, we take the convention $\Phi(R) = 0$. Eliminating the kinetic energy between Eqs. (69), (70) and (73), we obtain for $D \neq 2$:

$$(74) \quad W = \frac{-D}{D + 2 - (D - 2)n} \left\{ (n + 1) V_D R^D p(R) - (n + 1) \frac{p(R)}{\rho(R)} M + \frac{GM^2}{(D - 2)R^{D-2}} \right\},$$

and for $D = 2$:

$$(75) \quad W = -(n + 1) \frac{GM^2}{8} - \frac{1}{2}(n + 1) \pi R^2 p(R) + \frac{1}{2}(n + 1) \frac{p(R)}{\rho(R)} M.$$

For complete polytropes for which $p(R_*)/\rho(R_*) = 0$, we obtain the D -dimensional generalization of the Betti-Ritter formula [14]:

$$(76) \quad W = \frac{-D}{D + 2 - (D - 2)n} \frac{GM^2}{(D - 2)R_*^{D-2}} \quad (D \neq 2),$$

$$(77) \quad W = -(n + 1) \frac{GM^2}{8} \quad (D = 2).$$

We note that for $D > 2$, the potential energy is infinite for $n = n_5$ (while the mass is finite). Returning to the general case, the total energy $E = K + W$ can be written for $D \neq 2$:

$$(78) \quad E = \frac{-1}{D + 2 - (D - 2)n} \left\{ \frac{D(4 - D)}{2(D - 2)} \left[\frac{GM^2}{R^{D-2}} - (n + 1)(D - 2) M \frac{p(R)}{\rho(R)} \right] - DV_D R^D (n + 1 - D) p(R) \right\},$$

and for $D = 2$:

$$(79) \quad E = -(n-1)\frac{GM^2}{8} - \frac{1}{2}(n-1)\pi R^2 p(R) + \frac{1}{2}(n+1)\frac{p(R)}{\rho(R)}M.$$

Expressing the pressure $p(R)$ in terms of the Lane-Emden function $\theta(\alpha)$ using Eqs. (14) and (24), using Eqs. (59) and (62) to eliminate the central density ρ_0 and the polytropic constant K (or temperature T), and introducing the Milne variables (49), we finally obtain for $D \neq 2$:

$$(80) \quad \Lambda \equiv -\frac{ER^{D-2}}{GM^2} = \frac{-1}{(D-2)n - (D+2)} \left[\frac{D(4-D)}{2(D-2)} \left(1 - \frac{D-2}{v_0} \right) + \frac{n+1-D}{n+1} \frac{u_0}{v_0} \right],$$

and for $D = 2$:

$$(81) \quad \Lambda = \frac{1}{8}(n-1) + \frac{1}{4} \frac{n-1}{n+1} \frac{u_0}{v_0} - \frac{1}{2v_0}.$$

For $D \leq 2$ and for ($D > 2, n < n_5$), the normalized box radius α is necessarily restricted by the inequality $\alpha \leq \xi_1$. For the limiting value $\alpha = \xi_1$, corresponding to a complete polytrope with radius $R_* = R$, we have

$$(82) \quad \Lambda(\xi_1) = \lambda_n,$$

with

$$(83) \quad \lambda_n = \frac{-D(4-D)}{2(D-2)[(D-2)n - (D+2)]} \quad (D \neq 2),$$

$$(84) \quad \lambda_n = \frac{1}{8}(n-1) \quad (D = 2).$$

Alternatively, for $\Lambda > \lambda_n$, $R_* < R$. We note finally that, for $D > 2$, Eq. (80) is undetermined for $n = n_5$. Calculating the kinetic energy $K = (D/2) \int p d^D \mathbf{r}$ with Eqs. (14), (24), (45), and using the Virial theorem (69) to obtain the potential energy, we find after simplification that

$$(85) \quad \Lambda_5 = \frac{D^2}{4}(4-D) \left[1 + \frac{\alpha^2}{D(D-2)} \right]^D \frac{1}{\alpha^{D+2}} \int_0^\alpha \frac{\xi^{D-1}}{\left[1 + \frac{\xi^2}{D(D-2)} \right]^D} d\xi - \frac{D}{2\alpha^2}.$$

For $D = 3$, the integral is explicitly given by

$$(86) \quad \int_0^\alpha \frac{\xi^2}{\left(1 + \frac{\xi^2}{3} \right)^3} d\xi = \frac{9\alpha(\alpha^2 - 3)}{8(\alpha^2 + 3)^2} + \frac{3\sqrt{3}}{8} \arctan\left(\frac{\alpha}{\sqrt{3}} \right).$$

We note that for $\alpha \rightarrow +\infty$, the energy diverges like $\Lambda_5 \sim (\pi\sqrt{3}/64)\alpha$ for $D = 3$.

2.5 The minimum temperature and minimum energy

The curve $\eta(\alpha)$ presents an extremum at points α_k such that $d\eta/d\alpha(\alpha_k) = 0$. Using Eqs. (66), (50) and (51), we find that this condition is equivalent to

$$(87) \quad u_0 = \frac{(D-2)n - D}{n-1} = u_s.$$

Therefore, the points where η is extremum are determined by the intersections between the solution curve in the (u, v) plane and the straight line defined by Eq. (87). The number of extrema depends on the value of D and n . It can be determined easily by a graphical construction using Figs. 1-4 (an explicit construction is made in Fig. 18; see also [23] for $D = 3$). For $D \leq 2$, $u_s < 0$ for $n > 1$ and $u_s > D$ for $n < 1$ so that there is no extremum (case A). For $2 < D \leq 10$, there is no extremum for $n \leq n_3$ (case A), there is one maximum for $n_3 < n \leq n_5$ (case B) and there is an infinity of extrema for $n > n_5$ (case C). They exhibit damped oscillations towards the value η_s corresponding to the singular solution (27). Asymptotically, the α_k follow a geometric progression $\alpha_k \sim \exp\{2k\pi/\sqrt{-\Delta}\}$ (see [23] for $D = 3$). For $D > 10$, there is no extremum for $n \leq n_3$ (case A), there is one maximum for $n_3 < n \leq n_5$ (case B), there is an infinity of extrema for $n_5 < n < n_-$ (case C) and there is no extremum for $n \geq n_-$ (case D). This last case corresponds to an overdamped evolution towards the value η_s (in our mechanical analogy of Sec. 2.2). For $n = n_5$, using Eq. (68), we find that the extremum is located at $\alpha_1 = \sqrt{D(D+2)}$. The parameter η is restricted by the inequalities (see Figs. 5-6)

$$(88) \quad \eta \leq \omega_n \quad (\text{case A}),$$

$$(89) \quad \eta \leq \eta(\alpha_1) \quad (\text{cases B and C}),$$

$$(90) \quad \eta \leq \eta_s \quad (\text{case D}).$$

These inequalities determine a maximum mass (for given T and R) or a minimum temperature (for given M and R) beyond which the system will either converge toward a complete polytrope with radius $R_* < R$ (if it is stable) or collapse. This dynamical evolution will be studied in Sec. 3 with the aid of the nonlinear Smoluchowski-Poisson system.

The curve $\Lambda(\alpha)$ presents an extremum at points α'_k such that $d\Lambda/d\alpha(\alpha'_k) = 0$. Using Eqs. (80), (50) and (51), we find that this condition is equivalent to

$$(91) \quad 2(n+1-D)u_0^2 + (n+1)(n+1-D)u_0v_0 + 2(D-n-1)(D-1)u_0 + \frac{1}{2}D(D-4)(n+1)u_0 + \frac{1}{2}D(D-4)(n+1)v_0 + \frac{1}{2}D(D-4)(2-D)(n+1) = 0.$$

We can check that the point (u_s, v_s) is a solution of this equation. On the other hand, $v_0 = D-2$ for $u_0 = 0$ and $v_0 \sim -2u_0/(n+1)$ for $u_0 \rightarrow \pm\infty$. Finally, $v_0 \rightarrow \infty$ for $u_0 \rightarrow u_*$ where

$$(92) \quad u_* = \frac{D(4-D)}{2(n+1-D)}.$$

More precisely, for $u_0 \rightarrow u_*$, we have

$$(93) \quad (u_0 - u_*)v_0 \sim \frac{D(D-4)(D-2)}{2(n+1)(D-n-1)^2}(n - n_{3/2})(n - n_5) \equiv \Delta_2(n).$$

The two roots of $\Delta_2(n)$ are $n = n_{3/2} = D/2$ and $n = n_5$. They coincide at the particular dimension $D = 2(1 + \sqrt{2})$. We note also that $u_* = 0$ for $D = 4$. For $D > 2$ and $n = D-1$, Eq. (91) reduces to $u + v = D-2$.

The points where $\Lambda(\alpha)$ is extremum are determined by the intersections between the solution curve in the (u, v) plane and the curve defined by Eq. (91). The number of extrema can thus be

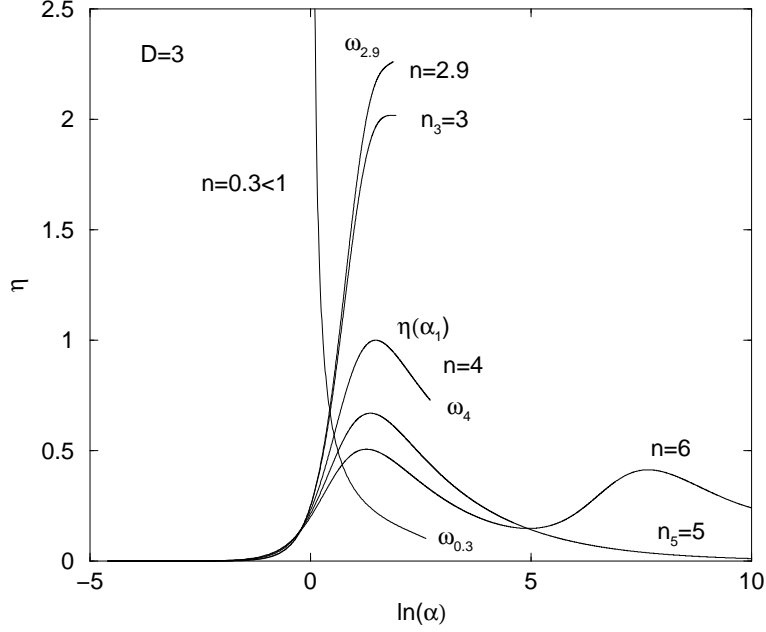


Figure 5: Mass-density profiles for polytropic configurations in a space of dimension $2 < D < 10$ (specifically $D = 3$). A mass peak appears for the first time for the index $n_3 = 3$. For $n > n_5 = 5$ the profile displays an infinity of peaks. For $n < 1$, η is a decreasing function of α . For $D \leq 2$, the $\eta(\alpha)$ curves are monotonic.

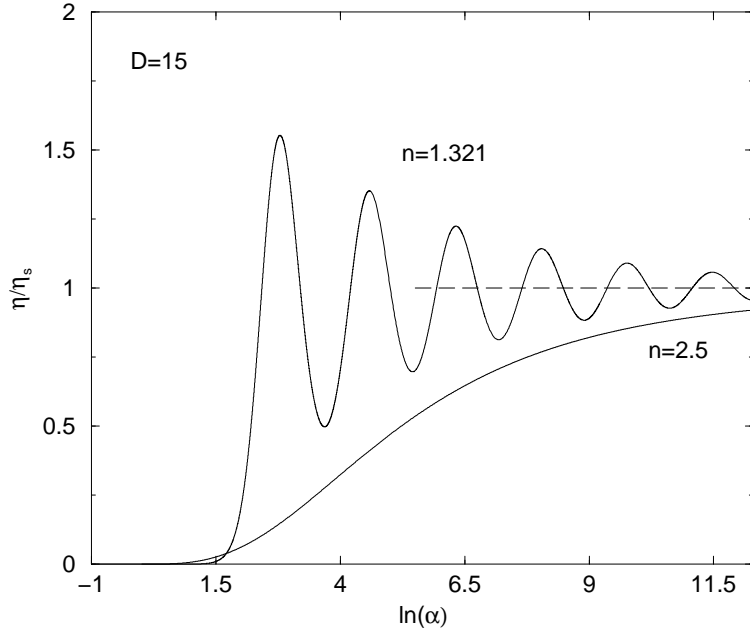


Figure 6: Mass-density profiles for polytropic configurations in a space of dimension $D > 10$ (specifically $D = 15$). For $n_5 < n < n_-$ (specifically $n = 1.321$) the profile displays an infinity of peaks. For $n > n_-$ (specifically $n = 2.5$) the function $\eta(\alpha) \rightarrow \eta_s$ for $\alpha \rightarrow +\infty$ without oscillating.

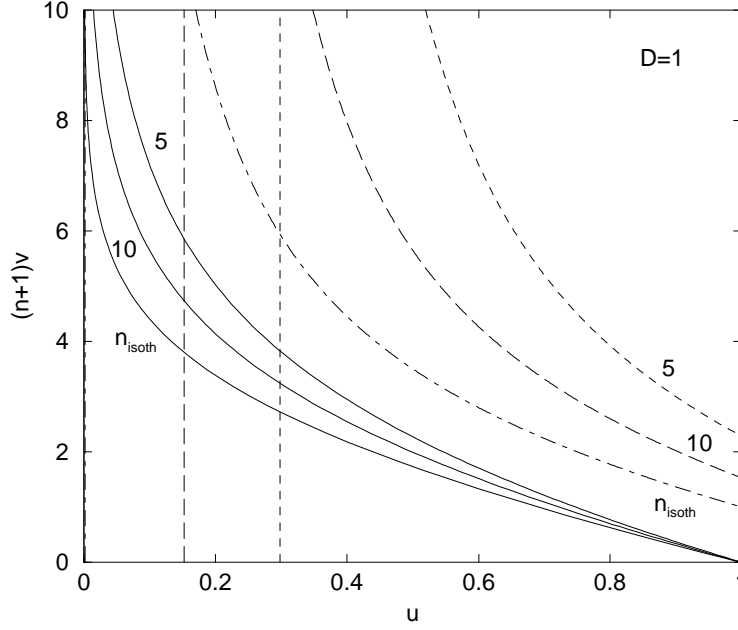


Figure 7: Graphical construction determining the extrema of $\Lambda(\alpha)$ for $D < 2$ (specifically $D = 1$). The solid lines correspond to the solution curves and the dashed lines to the curves defined by Eq. (91). The curves are labeled by the value of the polytropic index n . The vertical lines correspond to the asymptote $u = u_*$. For $D < 2$, there is no intersection so that $\Lambda(\alpha)$ has no extremum.

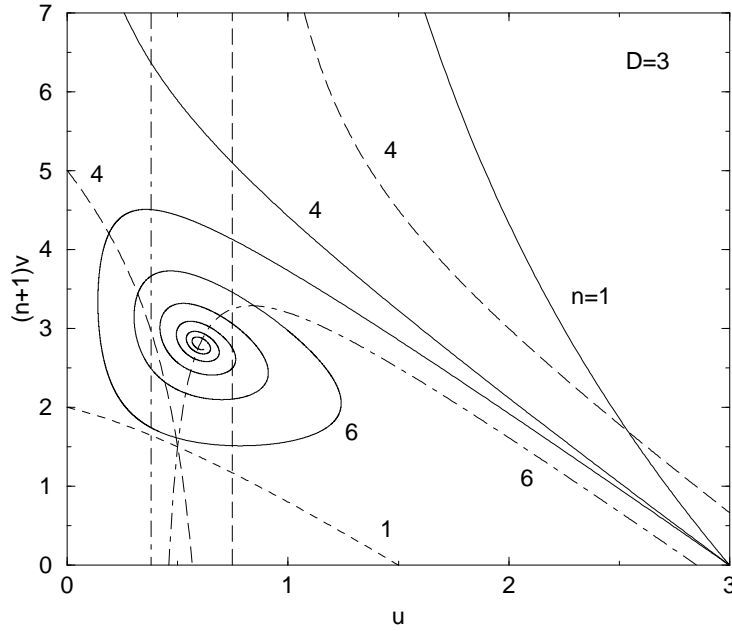


Figure 8: Same as Fig. 7 for $2 < D < 4$ (specifically $D = 3$). The geometrical construction changes for $n = D/2$, $n = D - 1$ and $n = n_5$. Typical cases are represented.

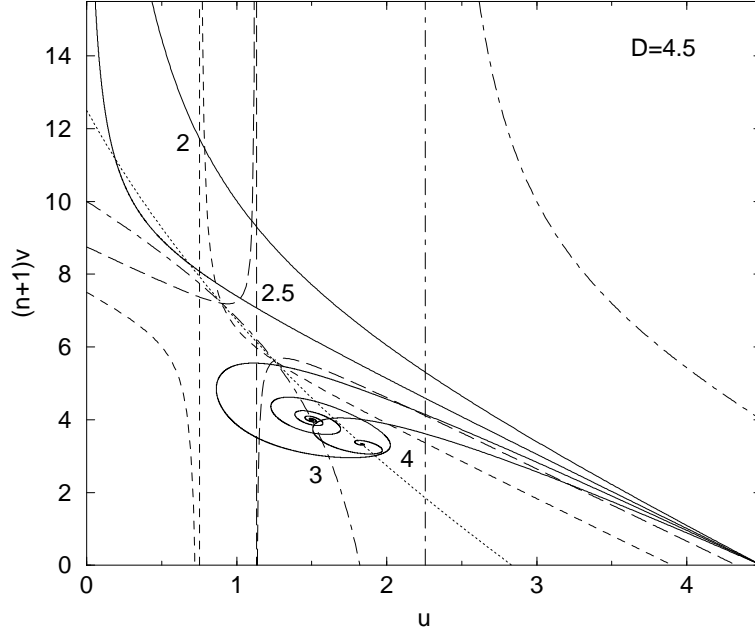


Figure 9: Same as Fig. 7 for $4 < D < 2(1 + \sqrt{2})$ (specifically $D = 4.5$). The geometrical construction changes for $n = D/2$, $n = n_5$ and $n = D - 1$. Typical cases are represented. The indices label both the solid curve and the closest broken curve.

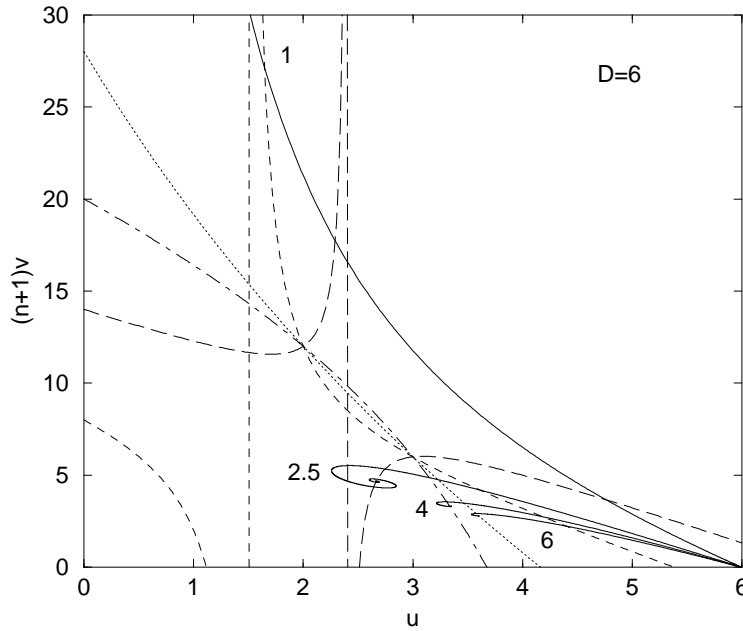


Figure 10: Same as Fig. 7 for $2(1 + \sqrt{2}) < D < 10$ (specifically $D = 6$). The geometrical construction changes for $n = n_5$, $n = D/2$ and $n = D - 1$. Typical cases are represented. The indices label both the solid curve and the closest broken curve.

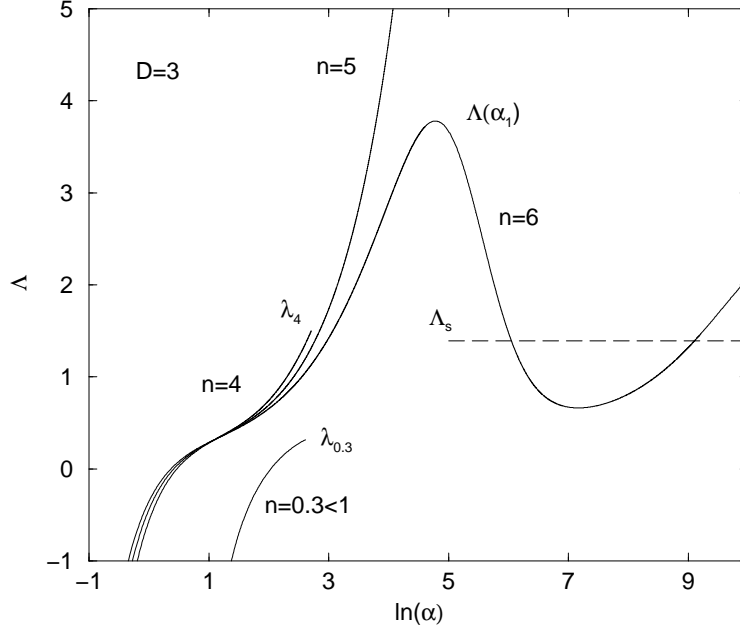


Figure 11: Evolution of the energy along the series of equilibria (parameterized by α) for $2 < D < 4$ (specifically $D = 3$). For $n < n_5 = 5$, the curve has no extremum. For $D \leq 2$, the $\Lambda(\alpha)$ curves are monotonic.

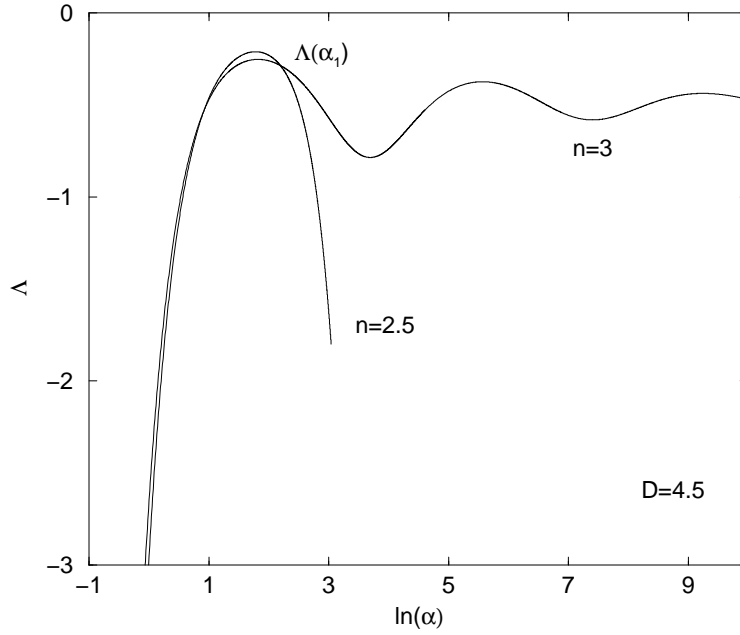


Figure 12: Evolution of the energy along the series of equilibria (parameterized by α) for $4 < D < 10$ (specifically $D = 4.5$). For $n < n_5$, the curve has one maximum. For $D > 10$, the $\Lambda(\alpha)$ curves are similar to the $\eta(\alpha)$ curves in Fig. 6.

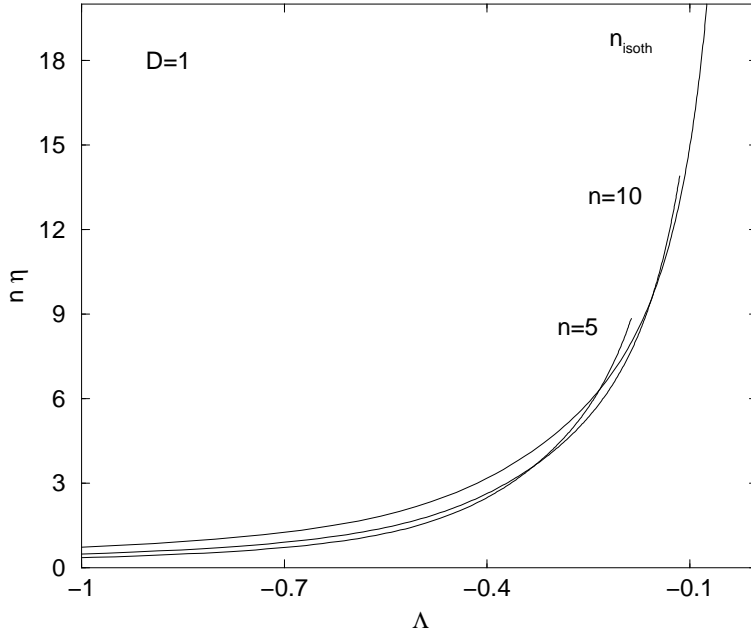


Figure 13: Generalized caloric curve for $D < 2$ (specifically $D = 1$). Note that according to Eq. (76), the potential energy is necessarily positive for $D < 2$, so the region $\Lambda \geq 0$ is forbidden.

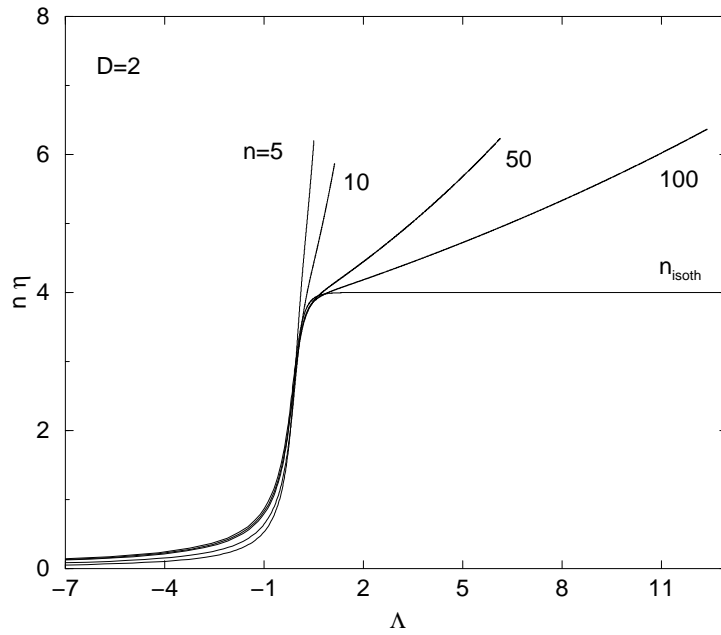


Figure 14: Generalized caloric curve for $D = 2$.

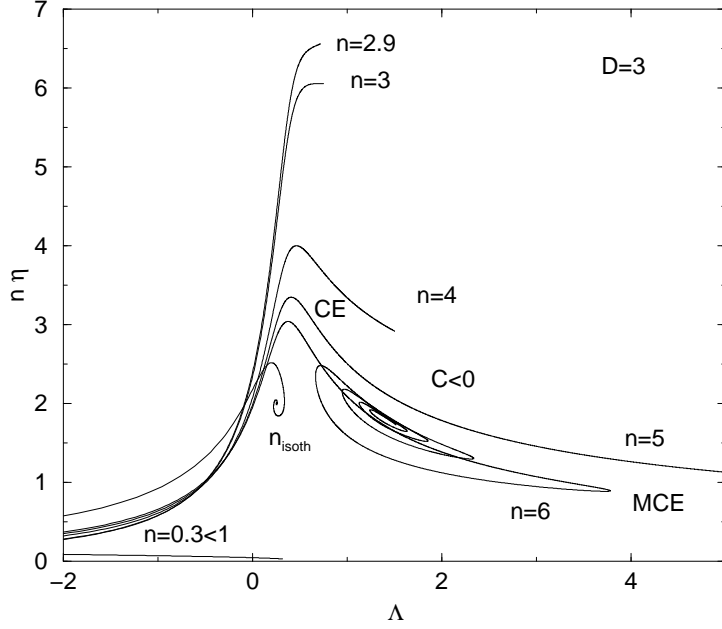


Figure 15: Generalized caloric curve for $2 < D < 4$ (specifically $D = 3$). For $n_3 < n < n_5$ (specifically $n_3 = 3$ and $n_5 = 5$) the inverse temperature presents a maximum but not the energy. For $n > n_3$ there exists a region of negative (generalized) specific heats $C < 0$ in the microcanonical ensemble.

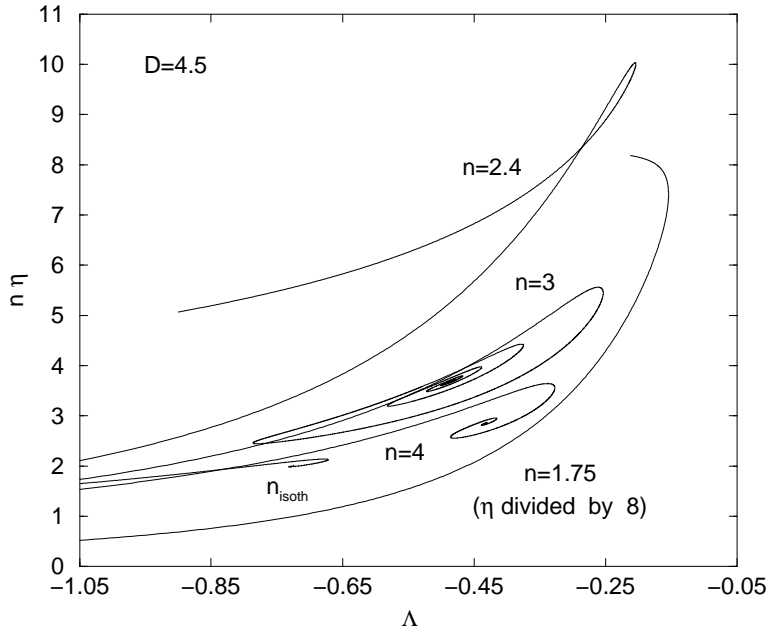


Figure 16: Generalized caloric curve for $4 < D < 10$ (specifically $D = 4.5$). For $n < n_3$ (specifically $n_3 = 1.8$) the energy presents a minimum but not the inverse temperature. This implies that equilibrium states with positive as well as negative specific heats ($C \sim \frac{q}{n-1} \frac{d\Lambda}{d\eta}$) are stable in the canonical ensemble. Although this result is mathematically correct regarding the maximization problem described in Sec. 2.1, it is at variance with usual thermodynamics where negative specific heats are forbidden in the canonical ensemble. Therefore, it constitutes a thermodynamical anomaly in our *thermodynamical analogy* [16]. For $n_3 < n < n_5$ (specifically $n_5 = 2.6$) both the energy and the inverse temperature present an extremum.

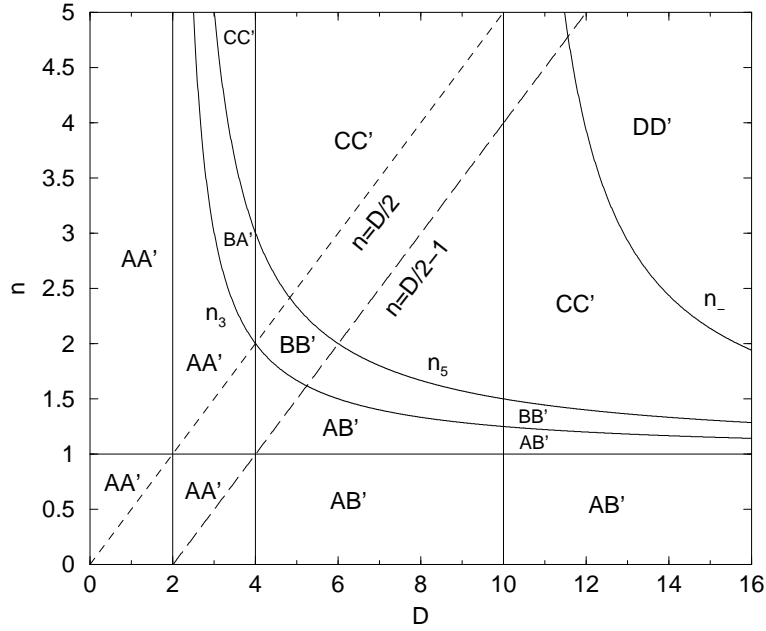


Figure 17: This figure summarizes the structure of the caloric curve as a function of the dimension D and the polytropic index n . The symbols are defined in the text. If we limit ourselves to $n \geq D/2$ (stellar polytropes), the region AB' showing a thermodynamical anomaly is not accessible.

determined by a graphical construction using Figs. 1-4. This graphical construction depends on the values of D and n and the different cases are shown in Figs. 7-10. For $D < 2$, there is no extremum (case A'). For $2 < D < 4$, there is no extremum for $n < n_5$ (case A') and there is an infinity of extrema for $n > n_5$ (case C'). They exhibit damped oscillations toward the value Λ_s corresponding to the singular solution (27). For $4 < D < 10$, there is one maximum for $n < n_5$ (case B') and there is an infinity of extrema for $n > n_5$ (case C'). For $D > 10$ there is one maximum for $n < n_5$ (case B'), there is an infinity of extrema for $n_5 < n < n_-$ (case C'), and there is no extremum for $n > n_-$ (case D'). This last case corresponds to an overdamped evolution towards the value Λ_s . The appearance of a maximum for $n < n_5$ when $D > 4$ was a surprise in view of preceding analysis for $D = 3$ [21, 23, 20]. The parameter Λ is restricted by the inequalities (see Figs. 11 and 12)

$$(94) \quad \Lambda \leq \lambda_n \quad (\text{case } A'),$$

$$(95) \quad \Lambda < \Lambda(\alpha_1) \quad (\text{cases } B' \text{ and } C'),$$

$$(96) \quad \Lambda \leq \Lambda_s \quad (\text{case } D').$$

These inequalities determine a minimum energy (for given M and R) below which the system will either converge toward a complete polytrope with radius $R_* < R$ (if it is stable) or collapse.

In Figs. 13-16, we have plotted the generalized caloric curve $\Lambda - \eta$, giving the inverse temperature as a function of the energy, for different dimensions D and polytropic index n . This extends the results of our previous analysis in $D = 3$ [23]. The number of turning points as a function of D and n is recapitulated in Fig. 17.

2.6 The generalized thermodynamical stability

We now come to the generalized thermodynamical stability problem. We shall say that a polytrope is stable if it corresponds to a maximum of Tsallis entropy (free energy) at fixed mass and energy (temperature) in the microcanonical (canonical) ensemble. The stability analysis has already been performed for $D = 3$ [21, 23, 22, 20] and is extended here to a space of arbitrary dimension.

We start by the canonical ensemble which is simpler in a first approach. A polytropic distribution is a local *maximum* of free energy at fixed mass and temperature if, and only if, the second order variations (see Appendix B)

$$(97) \quad \delta^2 J = -\frac{1}{2}\beta \left\{ \frac{n+1}{n} \int \frac{p}{\rho^2} (\delta\rho)^2 d^D \mathbf{r} + \int \delta\rho \delta\Phi d^D \mathbf{r} \right\},$$

are negative for any perturbation $\delta\rho$ that conserves mass, i.e.

$$(98) \quad \int \delta\rho d^D \mathbf{r} = 0.$$

This is the condition of (generalized) thermodynamical stability in the canonical ensemble. Introducing the function $q(r)$ by the relation

$$(99) \quad \delta\rho = \frac{1}{S_D r^{D-1}} \frac{dq}{dr},$$

and integrating by parts, we can put the second order variations of free energy in the quadratic form

$$(100) \quad \delta^2 J = \frac{1}{2}\beta \int_0^R dr q \left[K\gamma \frac{d}{dr} \left(\frac{\rho^{\gamma-2}}{S_D r^{D-1}} \frac{d}{dr} \right) + \frac{G}{r^{D-1}} \right] q.$$

The second order variations of free energy can be positive (implying instability) only if the differential operator which occurs in the integral has positive eigenvalues. We need therefore to consider the eigenvalue problem

$$(101) \quad \left[K\gamma \frac{d}{dr} \left(\frac{\rho^{\gamma-2}}{S_D r^{D-1}} \frac{d}{dr} \right) + \frac{G}{r^{D-1}} \right] q_\lambda(r) = \lambda q_\lambda(r).$$

with $q_\lambda(0) = q_\lambda(R) = 0$ in order to satisfy the conservation of mass. If all the eigenvalues λ are negative, the polytrope is a maximum of free energy. If at least one eigenvalue is positive, the polytrope is an unstable saddle point. The point of marginal stability in the series of equilibria is determined by the condition that the largest eigenvalue is equal to zero ($\lambda = 0$). We thus have to solve the differential equation

$$(102) \quad K\gamma \frac{d}{dr} \left(\frac{\rho^{\gamma-2}}{S_D r^{D-1}} \frac{dF}{dr} \right) + \frac{GF}{r^{D-1}} = 0,$$

with $F(0) = F(R) = 0$. Introducing the dimensionless variables defined previously, we can rewrite this equation in the form

$$(103) \quad \frac{d}{d\xi} \left(\frac{\theta^{1-n}}{\xi^{D-1}} \frac{dF}{d\xi} \right) + \frac{nF}{\xi^{D-1}} = 0,$$

with $F(0) = F(\alpha) = 0$. If

$$(104) \quad \mathcal{L} \equiv \frac{d}{d\xi} \left(\frac{\theta^{1-n}}{\xi^{D-1}} \frac{d}{d\xi} \right) + \frac{n}{\xi^{D-1}}$$

denotes the differential operator occurring in Eq. (103), we can check by using the Emden Eq. (25) that

$$(105) \quad \mathcal{L}(\xi^{D-1}\theta') = (n-1)\theta', \quad \mathcal{L}(\xi^D\theta^n) = [(2-D)n + D]\theta'.$$

Therefore, the general solution of Eq. (103) satisfying the boundary conditions at $\xi = 0$ is

$$(106) \quad F(\xi) = c_1 \left[\xi^D \theta^n + \frac{(D-2)n - D}{n-1} \xi^{D-1} \theta' \right].$$

Using Eq. (106) and introducing the Milne variables (49), the condition $F(\alpha) = 0$ can be written

$$(107) \quad u_0 = \frac{(D-2)n - D}{n-1} = u_s.$$

This relation determines the points at which a new eigenvalue becomes positive ($\lambda = 0^+$). Comparing with Eq. (87), we see that a mode of stability is lost each time that η is extremum in the series of equilibria, in agreement with the turning point criterion of Katz [25] in the canonical ensemble. When the curve $\eta(\alpha)$ is monotonic (cases *A* and *D*), the system is always stable because it is stable at low density contrasts ($\alpha \rightarrow 0$) and no change of stability occurs afterward. When the curve $\eta(\alpha)$ presents extrema (cases *B* and *C*), the series of equilibria becomes unstable at the point of minimum temperature (or maximum mass) α_1 . In Fig. 15, this corresponds to a point of infinite specific heat $C = dE/dT \rightarrow \infty$, just before entering the region of negative specific heats $C < 0$. When the curve $\eta(\alpha)$ presents several extrema (case *C*), secondary modes of instability appear at values $\alpha_2, \alpha_3, \dots$ (see [23] in $D = 3$). We note that complete polytropes are stable in the canonical ensemble if $D \leq 2$ and if ($D > 2$, $n \leq n_3$). They are unstable otherwise. In the *thermodynamical analogy* developed in [23, 20], this is a condition of nonlinear dynamical stability for gaseous polytropes with respect to the Jeans-Euler equations. In particular, the self-gravitating Fermi gas at zero temperature (a classical white dwarf star) is dynamically stable if $n_{3/2} < n_3$, i.e. $D < 4$.

According to Eq. (99), the perturbation profile that triggers a mode of instability at the critical point $\lambda = 0$ is given by

$$(108) \quad \frac{\delta\rho}{\rho_0} = \frac{1}{S_D \xi^{D-1}} \frac{dF}{d\xi},$$

where $F(\xi)$ is given by Eq. (106). Introducing the Milne variables (49), we get

$$(109) \quad \frac{\delta\rho}{\rho} = \frac{nc_1}{S_D} (v_s - v).$$

The density perturbation $\delta\rho$ becomes zero at point(s) ξ_i such that $v(\xi_i) = v_s$. The number of nodes is therefore given by the number of intersections between the solution curve in the (u, v) plane and the line $v = v_s$. It can be determined by straightforward graphical constructions using Figs. 1-4. When the solution curve is monotonic (case *B*), the density perturbation

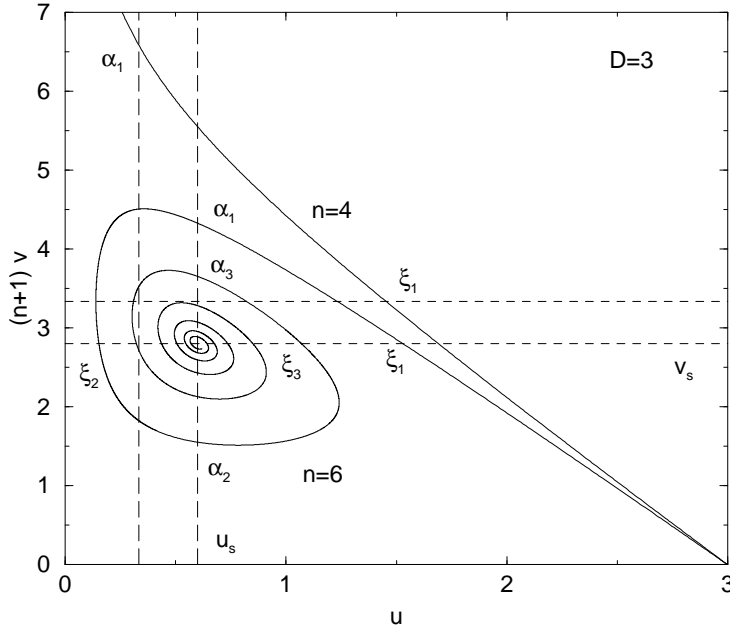


Figure 18: Location of the turning points of temperature in the (u, v) plane for systems with dimension $2 < D < 10$ (specifically $D = 3$). The line $u = u_s$ determines the extrema of η and the line $v = v_s$ determines the nodes of the density profiles that trigger the instabilities in the canonical ensemble.

profile has only one node. In particular, for $n = n_5$, the perturbation profile at the point of marginal stability is given by

$$(110) \quad \frac{\delta\rho}{\rho} = \frac{(D+2)c_1}{2S_D} \frac{D(D-2) - \xi^2}{D(D-2) + \xi^2}.$$

It vanishes for $\xi_{(1)} = \sqrt{D(D-2)}$. When the solution curve forms a spiral (case C), the density perturbation $\delta\rho$ corresponding to the k -th mode of instability has k zeros $\xi_1, \xi_2, \dots, \xi_k < \alpha_k$. In particular, the first mode of instability has only *one* node. For high modes of instability, the zeros asymptotically follow a geometric progression with ratio $1 : \exp\{2\pi/\sqrt{-\Delta}\}$ (see Ref. [23] for $D = 3$).

In the microcanonical ensemble, a polytrope is a maximum of entropy at fixed mass and energy if, and only if, the second order variations (see Appendix B)

$$(111) \quad \delta^2 S = \beta \left\{ -\frac{1}{2}\gamma \int p \frac{(\delta\rho)^2}{\rho^2} d^D \mathbf{r} - \frac{1}{2} \int \delta\rho \delta\Phi d^D \mathbf{r} - \frac{2n}{D(2n-D)} \frac{1}{\int p d^D \mathbf{r}} \left[\int \left(\Phi + \frac{D}{2}\gamma \frac{p}{\rho} \right) \delta\rho d^D \mathbf{r} \right]^2 \right\},$$

are negative for any variation $\delta\rho$ that conserves mass to first order (the conservation of energy has already been taken into account in obtaining Eq. (111)). Now, using Eq. (99) and integrating by parts, the second variations of entropy can be put in a quadratic form

$$(112) \quad \delta^2 S = \int_0^R \int_0^R dr dr' q(r) K(r, r') q(r'),$$

with

$$(113) \quad K(r, r') = -\frac{2n}{D(2n-D)} \frac{1}{\int p d^D \mathbf{r}} \left(\Phi + \frac{D}{2} K \gamma \rho^{\gamma-1} \right)'(r) \left(\Phi + \frac{D}{2} K \gamma \rho^{\gamma-1} \right)'(r') \\ + \frac{1}{2} \delta(r-r') \left[K \gamma \frac{d}{dr} \left(\frac{\rho^{\gamma-2}}{S_D r^{D-1}} \frac{d}{dr} \right) + \frac{G}{r^{D-1}} \right].$$

The problem of stability can therefore be reduced to the study of the eigenvalue equation

$$(114) \quad \int_0^R dr' K(r, r') q_\lambda(r') = \lambda q_\lambda(r),$$

with $q_\lambda(0) = q_\lambda(R) = 0$. The point of marginal stability ($\lambda = 0$) will be determined by solving the differential equation

$$(115) \quad K \gamma \frac{d}{dr} \left(\frac{\rho^{\gamma-2}}{S_D r^{D-1}} \frac{dF}{dr} \right) + \frac{GF}{r^{D-1}} = \frac{K \gamma^2}{Dn S_D} (2n-D) V \rho^{\gamma-2} \frac{d\rho}{dr},$$

with

$$(116) \quad V = \frac{\int_0^R \rho^{\gamma-2} \frac{d\rho}{dr} F dr}{\int_0^R \rho^\gamma r^{D-1} dr}.$$

In arriving at this expression, we have used the relation

$$(117) \quad \left(\Phi + \frac{D}{2} K \gamma \rho^{\gamma-1} \right)' = \frac{K \gamma}{2n} (D-2n) \rho^{\gamma-2} \frac{d\rho}{dr},$$

which results from the condition of hydrostatic equilibrium (20) with the polytropic equation of state (14). Introducing the dimensionless variables defined previously, Eqs. (115) and (117) can be rewritten

$$(118) \quad \frac{d}{d\xi} \left(\frac{\theta^{1-n}}{\xi^{D-1}} \frac{dF}{d\xi} \right) + \frac{nF}{\xi^{D-1}} = \chi \theta',$$

with

$$(119) \quad \chi = \frac{1}{D} (n+1)(2n-D) \frac{\int_0^\alpha \theta' F d\xi}{\int_0^\alpha \theta^{n+1} \xi^{D-1} d\xi},$$

and $F(0) = F(\alpha) = 0$. Using the identities (105), we can check that the general solution of Eq. (118) satisfying the boundary conditions for $\xi = 0$ and $\xi = \alpha$ is

$$(120) \quad F(\xi) = \frac{\chi}{(n-1)u_0 + D - (D-2)n} (\xi^D \theta^n + u_0 \xi^{D-1} \theta').$$

The point of marginal stability is then obtained by substituting the solution (120) in Eq. (119). Using the identities (see Appendix C)

$$(121) \quad \int_0^\alpha \xi^{D-1} (\theta')^2 d\xi = \frac{\alpha^D \theta'(\alpha)^2}{D+2-(D-2)n} \left(n+1 + 2 \frac{u_0}{v_0} - \frac{2D}{v_0} \right),$$

$$(122) \quad \int_0^\alpha \theta^{n+1} \xi^{D-1} d\xi = \frac{\alpha^D \theta'(\alpha)^2}{D+2-(D-2)n} \left(n+1 + 2 \frac{u_0}{v_0} - \frac{(D-2)(n+1)}{v_0} \right),$$

$$(123) \quad \int_0^\alpha \theta^n \theta' \xi^D d\xi = \frac{\alpha^D \theta'(\alpha)^2}{D+2-(D-2)n} \left(-D - (D-2) \frac{u_0}{v_0} + \frac{D(D-2)}{v_0} \right),$$

which result from simple integrations by parts and from the properties of the Lane-Emden equation (25), it is found that the point of marginal stability is determined by the condition (91). Therefore, the series of equilibria becomes unstable at the point of minimum energy in agreement with the turning point criterion of Katz [25] in the microcanonical ensemble. When the curve $\Lambda(\alpha)$ is monotonic (cases A' and D'), the system is always stable. When the curve $\Lambda(\alpha)$ presents extrema (cases B' and C'), the series of equilibria becomes unstable at the point of minimum energy α'_1 . In Fig. 15, this corresponds to the point where the specific heat $C = dE/dT = 0$, passing from negative to positive values. Note that the branch of negative specific heats between CE and MCE is stable in the microcanonical ensemble although it is unstable in the canonical ensemble. When the curve $\Lambda(\alpha)$ presents several extrema (case C'), secondary modes of instability appear at values $\alpha'_2, \alpha'_3, \dots$. We note that complete polytropes (with $n < n_5$ if $D > 2$) are stable in the microcanonical ensemble if $D \leq 4$ (and unstable if $D > 4$). Owing to the *thermodynamical analogy*, this is a condition of nonlinear dynamical stability for stellar polytropes with respect to the Vlasov equation [20]. Since the caloric curve is monotonic in $D = 2$, we also conclude that polytropic vortices [16] are always nonlinearly dynamically stable with respect to the 2D Euler equation.

According to Eqs. (108) and (120), the perturbation profile that triggers a mode of instability at the critical point $\lambda = 0$ is given by

$$(124) \quad \frac{\delta\rho}{\rho} = \frac{\chi}{S_D} \frac{1}{(n-1)u_0 + D - (D-2)n} (D - nv - u_0),$$

where we have used the Emden equation (25) and introduced the Milne variables (49). The number of nodes in the perturbation profile can be determined by a graphical construction similar to the one described in Refs. [26, 3] for $n = \infty$ (isothermal case).

3 Dynamics of self-gravitating Langevin particles in dimension D

3.1 The nonlinear Smoluchowski-Poisson system

We now consider the dynamics of a system of self-gravitating Langevin particles in a space of dimension D . To simplify the problem, we consider the high friction limit $\xi \rightarrow +\infty$, where ξ is the friction coefficient [2]. In that case, the evolution of the density is governed by the Smoluchowski equation [9]

$$(125) \quad \frac{\partial\rho}{\partial t} = \nabla \left[\nabla(D\rho) + \frac{1}{\xi} \rho \nabla\Phi \right],$$

coupled to the Newton-Poisson equation (4). In the usual case [2, 3], the diffusion coefficient D is constant and the condition that the Boltzmann distribution $\rho \sim e^{-\Phi/T}$ is a stationary solution of Eq. (125) leads to the Einstein relation $\xi D = T$. Furthermore, it can be shown [2] that the SP system increases the free energy (6) constructed with the Boltzmann entropy. We want to consider here a more general situation in which the diffusion coefficient D depends on the density ρ while the drift coefficient ξ is still constant. In the absence of drift, this

would lead to a situation of *anomalous diffusion*. In the presence of a drift, this leads to a notion of generalized thermodynamics. Indeed, writing the diffusion coefficient in the form $D(\rho) = \frac{1}{\xi}p(\rho)/\rho$, we obtain the generalized Smoluchowski equation proposed in [16]

$$(126) \quad \frac{\partial \rho}{\partial t} = \nabla \left[\frac{1}{\xi} (\nabla p + \rho \nabla \Phi) \right].$$

In Ref. [16], it is shown that generalized Smoluchowski equations of this type satisfy a form of H -theorem. The Lyapunov functional increasing monotonically with time is

$$(127) \quad J = - \int \rho \int_0^\rho \frac{p(\rho')}{\rho'^2} d\rho' d^D \mathbf{r} - \frac{1}{2} \int \rho \Phi d^D \mathbf{r} + \text{Cst.}$$

This can be interpreted as a free energy associated with a generalized entropy. The generalized Smoluchowski equation (126) can be obtained from a Langevin equation of the form

$$(128) \quad \frac{d\mathbf{r}}{dt} = -\frac{1}{\xi} \nabla \Phi + \sqrt{\frac{2p(\rho)}{\xi \rho}} \mathbf{R}(t),$$

where $\mathbf{R}(t)$ is a white noise. Since the function in front of $\mathbf{R}(t)$ depends on (\mathbf{r}, \mathbf{v}) , the last term in Eq. (128) is a multiplicative noise. In this paper, we shall assume, for simplicity, that the function $D(\rho)$ is a power law and write $\xi D(\rho) = K \rho^{\gamma-1}$. Then, Eq. (125) can be rewritten as

$$(129) \quad \frac{\partial \rho}{\partial t} = \nabla \left[\frac{1}{\xi} (K \nabla \rho^\gamma + \rho \nabla \Phi) \right].$$

For this nonlinear Smoluchowski equation [19], the Lyapunov functional increasing monotonically with time is [16]

$$(130) \quad J = -\frac{K}{\gamma-1} \int (\rho^\gamma - \rho) d^D \mathbf{r} - \frac{1}{2} \int \rho \Phi d^D \mathbf{r}.$$

It can be interpreted as a free energy (6) associated with Tsallis entropy (5). In this context, the polytropic index γ plays the role of the q -parameter and the polytropic constant K plays the role of the temperature (see Ref. [16] for details and subtleties). Therefore, keeping K fixed corresponds to a canonical situation [23]. For $\gamma \rightarrow 1$, we recover the Boltzmann free energy studied in [2, 3].

The nonlinear Smoluchowski equation can be obtained from a variational principle, called Maximum Entropy Production Principle, by maximizing the rate of free energy \dot{J} for a fixed total mass M [1]. It is straightforward to check that the rate of free energy production can be put in the form

$$(131) \quad j = \int \frac{1}{\rho \xi} (K \nabla \rho^\gamma + \rho \nabla \Phi)^2 d^D \mathbf{r} \geq 0.$$

For a stationary solution, $\dot{J} = 0$, and we obtain a polytropic distribution which is a critical point of J at fixed M . Considering a small perturbation around equilibrium, we can establish the identity [16]:

$$(132) \quad \delta^2 \dot{J} = 2\lambda \delta^2 J \geq 0,$$

where λ is the growth rate of the perturbation defined such that $\delta \rho \sim e^{\lambda t}$. This relation shows that a stationary solution of the nonlinear Smoluchowski-Poisson (NSP) system is dynamically

stable for small perturbations ($\lambda < 0$) if and only if it is a local *maximum* of free energy ($\delta^2 J < 0$). In addition, it is shown in Ref. [16] that the eigenvalue problem determining the growth rate λ of the perturbation is similar to the eigenvalue problem (102) associated with the second order variations of free energy (they coincide for marginal stability). This shows the equivalence between dynamical and generalized thermodynamical stability for self-gravitating Langevin particles exhibiting anomalous diffusion (this result was obtained independently by Shiino [17]). This equivalence remain valid for more general functionals than the Boltzmann or the Tsallis entropies [16]. These functionals (127) arise when the diffusion coefficient is of the general form $D(\rho)$, not necessarily a power law. Finally, we note that the NSP system satisfies a form of Virial theorem [16]. For $D \neq 2$, it reads

$$(133) \quad \frac{1}{2}\xi \frac{dI}{dt} = 2K + (D - 2)W - Dp_b V,$$

where

$$(134) \quad I = \int \rho r^2 d^D \mathbf{r},$$

is the moment of inertia and p_b the pressure on the box (assumed uniform). For $D = 2$, the term $(D - 2)W$ is replaced by $-GM^2/2$. For a stationary solution $dI/dt = 0$, we recover the Virial theorem (69).

The Smoluchowski-Poisson system defined by Eqs. (125) (4) is essentially a toy model for self-gravitating particles because the high friction limit is not justified in general for astrophysical systems (except, possibly, for the formation of planetesimals in the solar nebula since the dust particles experience a friction with the gas [27]). However, it satisfies the first and second principles of thermodynamics (conservation of mass and energy/temperature and increase of entropy/free energy) like the more realistic Landau-Fokker-Planck or Jeans-Navier-Stokes equations. Therefore, on a qualitative point of view, it exhibits similar features and it has the great interest to be amenable to a full analytical description. On the other hand, the SP system also provides a simple model for the chemotactic aggregation of bacterial populations [10]. The name chemotaxis refers to the motion of organisms induced by chemical signals. In some cases, the biological organisms secrete a substance that has an attractive effect on the organisms themselves. This is the case for the bacteria *Escherichia coli*. In the simplest model, the bacteria have a diffusive motion and they also move systematically along the gradient of concentration of the chemical they secrete. Since the density $\Phi(\mathbf{r}, t)$ of the secreted substance is induced by the particles themselves, the drift is directed toward the region of higher density. This attraction triggers a self-accelerating process until a point at which aggregation takes place. If we assume in a first step that $\Phi(\mathbf{r}, t)$ is related to the bacterial density $\rho(\mathbf{r}, t)$ by a Poisson equation, this phenomenon can be modeled by the SP system. Now, it has been observed in many occasions in biology that the diffusion of the particles is anomalous [10]. This is a physical motivation to study the NSP system in which the diffusion coefficient is a power law of the density. In the following section, we show that the NSP system admits self-similar solutions describing the collapse of the self-gravitating Langevin gas or of the bacterial population. These theoretical results are confirmed in Sec. 4 where we numerically solve the NSP system.

3.2 Self-similar solutions of the nonlinear Smoluchowski-Poisson system

From now on, we set $M = R = G = \xi = 1$ without loss of generality. The equations of the problem become

$$(135) \quad \frac{\partial \rho}{\partial t} = \nabla(K\nabla\rho^\gamma + \rho\nabla\Phi),$$

$$(136) \quad \Delta\Phi = S_D\rho,$$

with boundary conditions

$$(137) \quad \frac{\partial\Phi}{\partial r}(0, t) = 0, \quad \Phi(1) = \frac{1}{2-D}, \quad K\frac{\partial\rho^\gamma}{\partial r}(1) + \rho(1) = 0,$$

for $D \neq 2$. For $D = 2$, we take $\Phi(1) = 0$ on the boundary. We restrict ourselves to spherically symmetric solutions. Integrating Eq. (136) once, we can rewrite the NSP system in the form of a single integrodifferential equation

$$(138) \quad \frac{\partial\rho}{\partial t} = \frac{1}{r^{D-1}} \frac{\partial}{\partial r} \left\{ r^{D-1} \left[(S_D\rho)^{1/n} \Theta \frac{\partial\rho}{\partial r} + \frac{\rho}{r^{D-1}} \int_0^r \rho(r') S_D r'^{D-1} dr' \right] \right\},$$

where we have set

$$(139) \quad \Theta \equiv \frac{K(1+n)}{nS_D^{1/n}} = \frac{1}{n\eta^{1-1/n}}.$$

The quantity Θ can be seen as a sort of generalized temperature (sometimes called a polytropic temperature [23]) and it reduces to the ordinary temperature T for $n \rightarrow +\infty$. In the canonical ensemble Θ is constant. We can also set up a microcanonical description in which $\Theta(t)$ depends on time in order to keep the total energy strictly constant:

$$(140) \quad E = \frac{D}{2} \frac{nS_D^{1/n}}{1+n} \int \Theta(t) \rho^{1+\frac{1}{n}} d^D\mathbf{r} + \frac{1}{2} \int \rho\Phi d^D\mathbf{r}.$$

In that case, the NSP system increases the entropy S instead of the free energy J . The two situations have been considered in the case of isothermal systems ($n \rightarrow +\infty$) in [1, 2, 3].

The NSP system is also equivalent to a single differential equation

$$(141) \quad \frac{\partial M}{\partial t} = \Theta \left(\frac{1}{r^{D-1}} \frac{\partial M}{\partial r} \right)^{1/n} \left[\frac{\partial^2 M}{\partial r^2} - \frac{D-1}{r} \frac{\partial M}{\partial r} \right] + \frac{M}{r^{D-1}} \frac{\partial M}{\partial r},$$

for the quantity

$$(142) \quad M(r, t) = \int_0^r \rho(r') S_D r'^{D-1} dr',$$

which represents the mass contained within the sphere of radius r . The appropriate boundary conditions are

$$(143) \quad M(0, t) = 0, \quad M(1, t) = 1.$$

It is also convenient to introduce the function $s(r, t) = M(r, t)/r^D$ satisfying

$$(144) \quad \frac{\partial s}{\partial t} = \Theta \left(r \frac{\partial s}{\partial r} + Ds \right)^{1/n} \left(\frac{\partial^2 s}{\partial r^2} + \frac{D+1}{r} \frac{\partial s}{\partial r} \right) + \left(r \frac{\partial s}{\partial r} + Ds \right) s.$$

For $n \rightarrow +\infty$, these equations reduce to those studied in Refs. [2, 3] in the isothermal case. We look for self-similar solutions of the form

$$(145) \quad \rho(r, t) = \rho_0(t) f \left(\frac{r}{r_0(t)} \right), \quad r_0 = \left(\frac{\Theta}{\rho_0^{1-1/n}} \right)^{1/2}.$$

The radius r_0 defined by the foregoing equation provides a typical value of the core radius of an incomplete polytrope (with $n > n_5$). It reduces to the King's radius [24] as $n \rightarrow +\infty$. In terms of the mass profile, we have

$$(146) \quad M(r, t) = M_0(t) g \left(\frac{r}{r_0(t)} \right), \quad \text{with} \quad M_0(t) = \rho_0 r_0^D,$$

and

$$(147) \quad g(x) = \int_0^x f(x') S_D x'^{D-1} dx'.$$

In terms of the function s , we have

$$(148) \quad s(r, t) = \rho_0(t) S \left(\frac{r}{r_0(t)} \right), \quad \text{with} \quad S(x) = \frac{g(x)}{x^D}.$$

Substituting the *ansatz* (148) into Eq. (144), and using the definition of r_0 in Eq. (145), we find that

$$(149) \quad \frac{d\rho_0}{dt} S - \frac{\rho_0}{r_0} \frac{dr_0}{dt} x S' = \rho_0^2 (x S' + D S)^{1/n} \left(S'' + \frac{D+1}{x} S' \right) + \rho_0^2 (x S' + D S) S,$$

where we have set $x = r/r_0$. We now assume that there exists α such that

$$(150) \quad \rho_0 \sim r_0^{-\alpha}.$$

Inserting this relation into Eq. (149), we find

$$(151) \quad \frac{d\rho_0}{dt} \left(S + \frac{1}{\alpha} x S' \right) = \rho_0^2 \left[(x S' + D S)^{1/n} \left(S'' + \frac{D+1}{x} S' \right) + (x S' + D S) S \right],$$

which implies that $(1/\rho_0^2)(d\rho_0/dt)$ is a constant that we arbitrarily set equal to α . This leads to

$$(152) \quad \rho_0(t) = \frac{1}{\alpha} (t_{coll} - t)^{-1},$$

so that the central density becomes infinite in a finite time t_{coll} . The scaling equation now reads

$$(153) \quad \alpha S + x S' = (x S' + D S)^{1/n} \left(S'' + \frac{D+1}{x} S' \right) + (x S' + D S) S.$$

For $x \rightarrow +\infty$, we have asymptotically

$$(154) \quad S(x) \sim x^{-\alpha}, \quad g(x) \sim x^{D-\alpha}, \quad f(x) \sim x^{-\alpha}.$$

In the canonical ensemble where Θ is constant, Eq. (145) and Eq. (150) lead to $\alpha = \alpha_n$, with

$$(155) \quad \alpha_n = \frac{2n}{n-1}.$$

Note that for $n \rightarrow \infty$, we recover the result of [3], $\alpha_\infty = 2$. Eq. (154) implies that for large x , $\rho \sim (D - \alpha)S > 0$, which enforces $\alpha < D$ (this also guarantees that the mass is finite at $t = t_{coll}$). The limit value $\alpha_n = D$ corresponds to $n = n_3$. Therefore, there is no scaling solution for $n < n_3$. This is consistent with our finding that the collapse occurs only for $n > n_3$. For $n < n_3$ and $\eta > \omega_n$, the system converges toward a complete polytrope with radius $R_* < 1$ which is stable (Sec. 2.6). For $n_3 < n < n_5$ and $\eta > \eta(\alpha_1)$, we can formally construct a complete polytrope with radius $R_* < 1$, but this structure is unstable (Sec. 2.6) so that the system undergoes gravitational collapse.

In the microcanonical ensemble, the value of $\alpha \geq \alpha_n$ cannot be obtained by dimensional analysis. It will be selected by the dynamics. In the case $n \rightarrow +\infty$, we have found in [3] that Eq. (153) for the scaling profile has physical solutions only for $2 \leq \alpha \leq \alpha_{\max}(D)$ (with $\alpha_{\max}(D=3) = 2.209733\dots$). For arbitrary n , such a $\alpha_{\max}(D, n) \geq \alpha_n$ also exists (see Sec. 4). It is easy to see that the maximum value for α leads to the maximum divergence of temperature and entropy. Therefore, it is natural to expect that the value α_{\max} will be selected by the dynamics except if some kinetic constraints forbid this natural evolution (see below). In fact, as already noted in [2], a value of $\alpha > \alpha_n$ poses problem with respect to the conservation of energy. We recall (and generalize) the argument below. According to Eqs. (145), (150) and (152), the (generalized) temperature behaves as

$$(156) \quad \Theta \sim \rho_0^{1-1/n-2/\alpha} \sim (t_{coll} - t)^{-(2/\alpha_n - 2/\alpha)},$$

and the kinetic energy (18) behaves as

$$(157) \quad K \sim \Theta \int_0^1 \rho^\gamma(r, t) r^{D-1} dr \sim \Theta (\rho_0 r_0^\alpha)^\gamma \times \int_{r_0}^1 r^{D-1-\gamma\alpha} dr \sim \Theta \int_{r_0}^1 r^{D-1-\gamma\alpha} dr.$$

First consider the case $n > n_5$. If $\alpha < D/\gamma$ (which is the case in practice since $\alpha_n < D/\gamma$ implies $n > n_5$), the integral is finite and the kinetic energy behaves as $K \sim \Theta$. Therefore, it *diverges* at t_{coll} for any $\alpha > \alpha_n$. On the other hand, the scaling contribution to the potential energy behaves as

$$(158) \quad W \sim \int_0^1 \frac{M^2(r, t)}{r^{D-1}} dr \sim (\rho_0 r_0^\alpha)^2 \times \int_{r_0}^1 r^{D+1-2\alpha} dr \sim \int_{r_0}^1 r^{D+1-2\alpha} dr.$$

If $\alpha < (D+2)/2$ (which is the case in practice since $\alpha_n < (D+2)/2$ implies $n > n_5$), the scaling part of W remains *finite* at t_{coll} . Energy conservation would then imply that $\alpha = \alpha_n$. In a first series of numerical experiments reaching moderately high values of the central density [2], we measured (by different methods) a scaling exponent $\alpha \simeq 2.2 > \alpha_\infty = 2$ (for the isothermal case $n = \infty$). Combined with the fact that the Smoluchowski-Poisson system must lead to a diverging entropy, we argued that α_{\max} is selected by the dynamics (while being careful not to rigorously reject the possibility that $\alpha = \alpha_\infty$). Then, in order to account for energy conservation, we proposed a heuristic scenario showing how subscaling contributions could

lead to the divergence of potential energy. In fact, the numerical simulations were not really conclusive in showing the divergence of temperature, as the expected exponent is very small ($2/\alpha_n - 2/\alpha_{\max} = 0.09491\dots$, for $D = 3$ and $n \rightarrow +\infty$). Recently, we have conducted a new series of numerical simulations allowing to achieve much higher values of density (see Sec. 4). These simulations tend to favor a value of $\alpha = \alpha_n$ leading to a finite value of the temperature at t_{coll} . However, the convergence to the value α_n is obtained for values of t very close to t_{coll} and, at intermediate times for which the temperature has not reached its asymptotic value, the numerical scaling function tends to display an *effective exponent* between 2 and α_{\max} . This situation is reminiscent of the ($D = 2, n = +\infty$) case studied in [3], although the situation is not exactly equivalent. Numerical simulations of the ($D = 3, n = +\infty$) case have been conducted independently by [8] and favor also a value of $\alpha = \alpha_n$. Note that there is no mathematical result proving that $\alpha = \alpha_n$ in the microcanonical situation, so this point remains an open problem.

For $n < n_5$, the kinetic and potential energies diverge in a consistent way as

$$(159) \quad K \sim \Theta \int_{r_0}^1 r^{D-1-\gamma\alpha} dr \sim \Theta r_0^{D-\gamma\alpha} \sim \rho_0^{2-(D+2)/\alpha},$$

$$(160) \quad W \sim \int_{r_0}^1 r^{D+1-2\alpha} dr \sim r_0^{D+2-2\alpha} \sim \rho_0^{2-(D+2)/\alpha}.$$

However, in the microcanonical ensemble, the system is expected to reach a confined polytrope state for $n < n_5$ and $\Lambda > \lambda_n$ since it is stable.

The previous discussion shows that the system has the *desire* to achieve a value of $\alpha > \alpha_n$ leading to a divergence of temperature and entropy. This is indeed a natural evolution in a thermodynamical sense. This is also consistent with the notion of *gravothermal catastrophe* introduced in the context of globular clusters [28, 29, 30]. However, the energy constraint (140) seems to prevent this natural evolution (we believe that the divergence of entropy occurs in the post-collapse regime [15]). This is related to the assumption that the temperature is *uniform* although this assumption clearly breaks down during the late stage of the collapse as already indicated in [1]. Therefore, we expect that if the temperature is not constrained to remain constant, the system will select a value of $\alpha > 2$ (we now focus on the case $n = \infty$) as in other models of microcanonical gravitational collapse [29, 30]. Below, we give a heuristic hint so as how this can happen. We consider the Smoluchowski equation

$$(161) \quad \frac{\partial \rho}{\partial t} = \nabla[\nabla(T\rho) + \rho\nabla\Phi],$$

where $T = T(\mathbf{r}, t)$ is now position dependant. In any model where the temperature $T(\mathbf{r}, t)$ satisfies a *local* conservation of energy, we expect the following scaling

$$(162) \quad T(r, t) = T_0(t)\theta\left(\frac{r}{r_0(t)}\right), \quad \text{with} \quad \theta(x) \sim x^{2-\alpha}, \quad \text{when} \quad x \rightarrow +\infty.$$

Such a scaling is indeed observed in the globular cluster model of [30]. The decay exponent is obtained by using the definition of $T_0 \sim \rho_0 r_0^2$ and the fact that the temperature at distances $r \gg r_0$ should be of order unity. The precise density and temperature profiles and the value of α depend on the model considered for the energy transport equation. It is not our purpose to discuss a precise model in the present paper and we postpone this study for a future work [31]. However, we can give an analytical argument showing why $\alpha > 2$ should now be selected in a unique way. Equation (162) shows that temperature scales as the potential Φ since

$$(163) \quad \Phi(r, t) = \Phi(1) - \int_r^1 s(r', t)r' dr' \approx \Phi(1) - \rho_0 r_0^2 \int_{r/r_0}^{1/r_0} S(x)x dx \approx -T_0 \int_{r/r_0}^{+\infty} S(x)x dx.$$

The scaling function for $\Phi(r, t)$ is then

$$(164) \quad \phi(x) = - \int_x^{+\infty} S(x')x' dx' \sim x^{2-\alpha}, \quad \text{when } x \rightarrow +\infty.$$

Eqs. (162), (163) and (164) imply that both the kinetic and potential energies remain bounded for all times $t \leq t_{coll}$, at least for $\alpha < (D+2)/2$, even if the central temperature $T_0(t)$ diverges. Indeed, the temperature increases in the core but the core mass goes to zero so that the kinetic energy of the core $\sim M_0 T_0$ goes to zero. On the other hand, the temperature remains of order unity in the halo leading to a finite kinetic energy in the halo. This ‘‘core-halo’’ structure for the temperature is more satisfactory than a model in which the temperature is uniform everywhere, even in the collapse phase (the necessity of considering heat transfers between the core and the halo was pointed out in [1]). In the absence of a precise equation for $T(r, t)$ (work in progress), we make the reasonable claim that the temperature and the potential energy are simply proportional in the core region as they exhibit a similar scaling relation. Defining $T_0(t)$ such that $\theta(0) = 1$, we end up with the hypothesis

$$(165) \quad \theta(x) = \frac{\phi(x)}{\phi(0)} = \frac{\lambda}{D} \int_x^{+\infty} S(x')x' dx',$$

with

$$(166) \quad \lambda = -\frac{D}{\phi(0)} = \frac{D}{\int_0^{+\infty} S(x')x' dx'}.$$

Using Eq. (165), we find that the scaling equation for $S(x)$ is now

$$(167) \quad \alpha S + xS' = \frac{\lambda}{D}\phi(x)\left(S'' + \frac{D+1}{x}S'\right) + \left(1 - \frac{\lambda}{D}\right)S(xS' + DS).$$

For a given λ , this equation is an eigenvalue problem in α . In the limit of large dimension and proceeding exactly along the line of [3], it can be seen that $S \sim O(D^{-1})$ and $\lambda \sim O(D^0)$. Using the method of [3], $S(x)$ and α can be computed easily up to order $O(D^{-1})$, as a function of λ and $z = DS(0)/2$. Now imposing the constraint of Eq. (166), this selects a *unique* value for α . After straightforward calculations (see [31] for details), we find a simple parametrization of λ and α as a function of $z = DS(0)/2 > 2$:

$$(168) \quad \alpha - 2 = \frac{4}{D}(1 - 2z^{-1}) + O(D^{-2}),$$

$$(169) \quad \lambda = 2(1 - z^{-1})(1 - 2z^{-1}) + O(D^{-1}),$$

which can be recast in the form

$$(170) \quad \alpha - 2 = \frac{2}{D}\left(\sqrt{1+4\lambda} - 1\right) + O(D^{-2}),$$

$$(171) \quad S(0) = \frac{8}{D}\left(3 - \sqrt{1+4\lambda}\right)^{-1} + O(D^{-2}).$$

Eq. (169) implies that for $\lambda \geq 2$ (up to order $O(D^{-1})$), there is no solution to the scaling equation, and that for $\lambda < 2$, there is a unique α corresponding to a physical solution. In general, the actual value of λ will be selected dynamically by an additional evolution equation for the temperature profile. However, assuming $\lambda \simeq 1$ is natural (although this point needs to be confirmed), since it corresponds naively to a local energy conservation condition

$$(172) \quad \frac{D}{2}T(r, t) \sim -\frac{1}{2}\Phi(r, t).$$

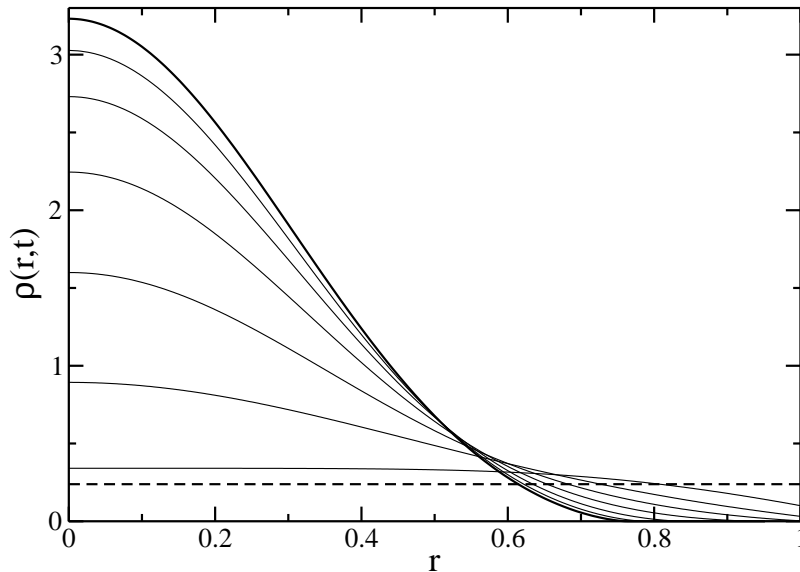


Figure 19: Evolution of the density profile $\rho(r, t)$ for $n = 3/2$ and $\Theta = 0.1$. The profile converges to a complete polytrope strictly confined inside the box (thick line). The dashed line is the initial uniform density profile.

In that case, we obtain

$$(173) \quad \alpha - 2 = \frac{2}{D} (\sqrt{5} - 1) + O(D^{-2}).$$

The above argument is a strong indication that if the uniform temperature constraint is abandoned, a non trivial value for $\alpha > 2$ will be selected. We conjecture that this eigenvalue will be close to $\alpha_{\max} \simeq 2.21$ as found in other models of microcanonical gravitational collapse with a non-uniform temperature [29, 30].

4 Numerical simulations

In this section, we illustrate numerically some of the theoretical results presented in the previous sections, but we restrain ourselves to $D = 3$.

We first consider the dynamics in the canonical ensemble (fixed Θ). In Fig. 19, we show the different steps of the formation of a self-confined polytrope of index $n = 3/2 < n_3 = 3$ (classical “white dwarf”). In this range of n , the system always converges to an equilibrium state. If $\eta < \omega_n$ the equilibrium state is confined by the box (incomplete polytrope) while for $\eta > \omega_n$ the density vanishes at $R_* < R$ (complete polytrope). In Fig. 20, we illustrate the collapse dynamics at low temperatures for $n = 4 \in [n_3, n_5]$ and $n = \infty > n_5 = 5$. This is compared to the predicted scaling profiles. The convergence to scaling is slower for $n = 4$ ($\alpha = 8/3$) than for $n = \infty$ ($\alpha = 2$). This is expected since, in the former case, $r_0 \sim \rho_0^{-1/\alpha}$ decreases more slowly as α is bigger. Thus, the scaling regime $r_0 \ll 1$ is reached in a slower way. For instance, for comparable final densities of order 10^6 , and for the considered temperatures, we find that the minimum r_0 obtained for $n = 4$ is roughly 4 times bigger than in the $n = \infty$ simulations. For $n = \infty$ and in the large D limit, we have shown in [3] that the scaling function $S(x)$ takes the form

$$(174) \quad S(x) = \frac{\alpha}{D} \left[1 + \left(1 - \frac{\alpha}{2z} \right) \left(\frac{x^2}{x_0^2} - 1 \right) \left(\frac{x^2}{x_1^2} + 1 \right)^{\frac{\alpha}{2}-1} \right]^{-1},$$

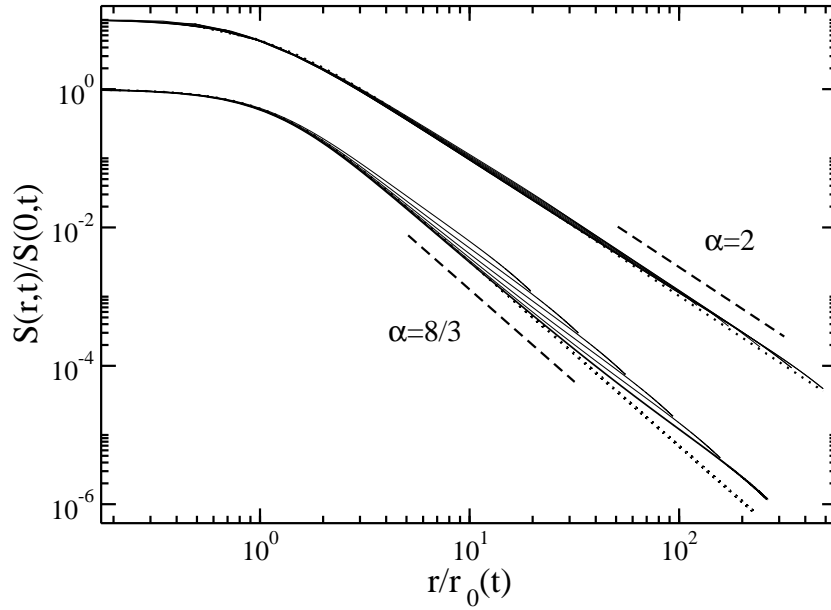


Figure 20: For $n = 4$ ($\alpha_4 = 8/3$) and $\Theta = 0.1$ (canonical description), we plot $S(r, t)/S(0, t)$ as a function of $r/r_0(t)$, where $r_0(t)$ is defined by Eq. (145), for different times corresponding to central densities in the range $2 \cdot 10^2 \sim 4 \cdot 10^5$ (bottom data collapse). This is compared to the scaling function obtained by solving Eq. (153) numerically (dotted line). The same is plotted in the case $n = \infty$ ($\alpha_\infty = 2$), for which the scaling profile is known analytically [3] : $S(x)/S(0) = (1 + x^2)^{-1}$ (upper data collapse). The two curves have been shifted for clarity. In the $n = \infty$ case, the asymptotic scaling profile (dotted line) is almost indistinguishable from the data collapse. Dashed lines have respective slopes $-8/3$ and -2 .

where x_0 is such that $S(x_0) = \alpha/D$. The quantities $z = DS(0)/2$ and $\alpha(z)$ have been exactly calculated in this limit. In the present case, and for a given n (yielding $\alpha_n = 2n/(n-1)$), we compute $S(0)$, by assuming the above functional form. The parameter x_0 , x_1 and $S(0)$ are numerically calculated by imposing the exact value for $S''(0)$ extracted from Eq. (153), as well as the two conditions that x_0 must satisfy (see [3] for more details). The comparison of this approximate theory with actual numerical data is satisfactory (see Fig. 21). Note that we have been unable to develop a large n perturbation theory in the same spirit as the large D expansion scheme derived in [3].

As explained in the previous section, the situation in the microcanonical ensemble (where $\Theta = \Theta(t)$ evolves with time in order to conserve energy) is less clear. Like in the case $n = \infty$ studied in [3], the scaling equation admits a physical solution for any $\alpha_n \leq \alpha \leq \alpha_{\max}(D, n)$. In Fig. 22, we plot $\alpha_{\max}(D = 3, n)$, as well as the corresponding value of $S(0)$, as a function of n . As explained previously, it is doubtful that a scaling actually develops with $\alpha > \alpha_n$ when the temperature is uniform. However, a *pseudo-scaling* should be observed with $\alpha \simeq \alpha_{\max}$. In Fig. 23, we present new simulations ($D = 3, n = \infty$) confirming that the observed scaling dynamics is better described by $\alpha = \alpha_{\max}$ than by $\alpha = 2$, in the time/density range achieved. Such a value of α implies that the temperature would diverge with a small exponent ($\Theta(t) \sim \rho_0(t)^{1-2/\alpha_{\max}}$, with $1 - 2/\alpha_{\max} = 0.09491\dots$). However, in the range of accessible densities $\rho_0 = 2 \cdot 10^{-1} \sim 10^6$, numerical data tend to suggest that the temperature converges to a finite value with an infinite derivative $\frac{d\Theta}{dt}(t_{\text{coll}}) = +\infty$ as $t \rightarrow t_{\text{coll}}$. This convergence of the temperature has been observed independently by [8]. Thus, we conclude that the system first develops an apparent scaling with $\alpha \lesssim \alpha_{\max}$, before slowly approaching the asymptotic

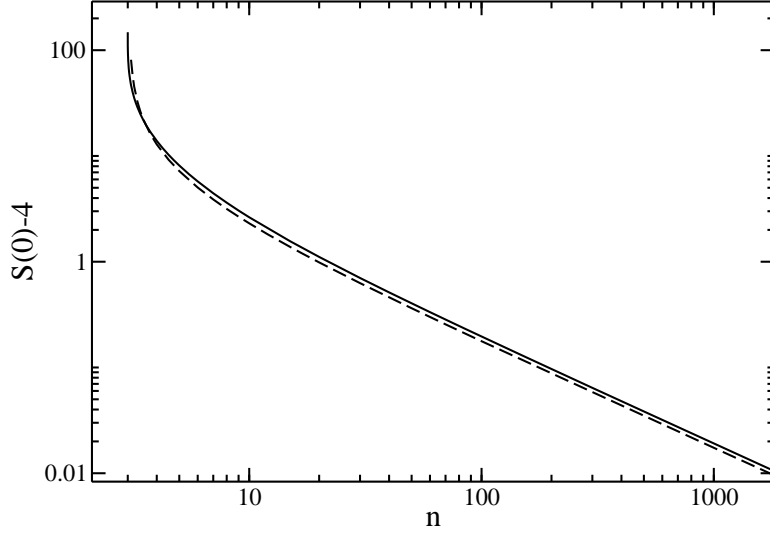


Figure 21: We plot $S(0)$ as a function of n (full line), and compare it to a simple theory explained in the text, which is inspired by the large D perturbation introduced in [3] (dashed line). Note that $S(0) \simeq 4 + C/n + O(n^{-2})$ for large n with $C \simeq 19$.

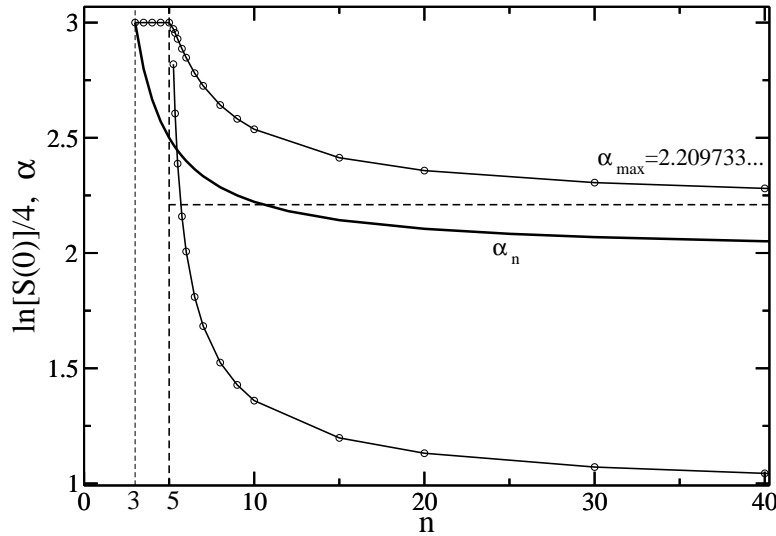


Figure 22: We plot $\alpha_{\max}(D = 3, n)$ as a function of n (top plot), as well as the associated value of $\frac{1}{4} \ln S(0)$ (bottom plot). The horizontal dashed line represents the asymptotic value of α_{\max} for $n \rightarrow +\infty$, and we find $\alpha_{\max}(D = 3, n) \approx \alpha_{\max}(D = 3, n = \infty) + C_3/n + O(n^{-2})$ for large n , with $C_3 \sim 2.7$. For $n \leq n_5 = 5$, $\alpha_{\max} = D^- = 3^-$ (strictly speaking, the scaling solution associated to $\alpha = D = 3$ does not exist below $n_5 = 5$). We observe that $\ln S(0) \sim (n - 5)^{-1/4}$ provides an excellent fit of $S(0)$ for $n \in [5, 10]$. We have also plotted $\alpha_n = 2n/(n - 1)$ (thick line). The scaling equation admits solutions for $\alpha_n \leq \alpha \leq \alpha_{\max}$. The two curves intersect when $\alpha_n = D$ which corresponds to $n = n_3$. There is no scaling collapse solution for $n \leq n_3$.

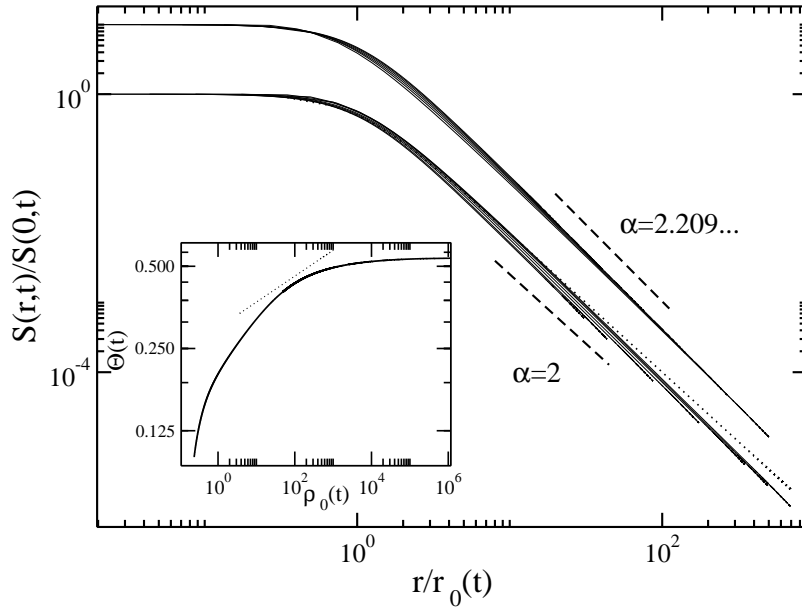


Figure 23: For $n = +\infty$ and $E = -0.45$ (microcanonical description), we plot $S(r, t)/S(0, t)$ as a function of $r/r_0(t)$ where $r_0(t) \sim \rho_0(t)^{1/\alpha}$, for times corresponding to central densities in the range $2 \cdot 10^2 \sim 4 \cdot 10^5$ (for comparison, our previous simulations [2] did not exceed $\rho_0 \sim 1000$). We try both values $\alpha_\infty = 2$ (bottom plot) and $\alpha = \alpha_{\max} = 2.209733\dots$ (top plot), and compare both data collapses to the associated scaling function (dotted lines). The two curves have been shifted for clarity. The scaling associated to α_{\max} is clearly more convincing than that for $\alpha = 2$, especially at large distances. However, our simulations also suggest that $\Theta(t) \sim \rho_0(t)^{1-2/\alpha_{\max}}$ does not diverge at t_{coll} (see the insert where a line of slope $1 - 2/\alpha_{\max} \approx 0.09491\dots$ has been drawn as a guide to the eye), so that the asymptotic scaling should correspond to $\alpha = 2$. This apparent “paradox” clearly shows that the convergence to the limit value $\alpha = \alpha_n$ is extremely slow, suggesting an intermediate pseudo-scaling regime with $\alpha_n \leq \alpha \leq \alpha_{\max}$.

scaling regime with $\alpha = 2$. In any case, it is clear that if the $\alpha = 2$ scaling is the relevant one, the scaling regime is approached much more slowly than in the canonical ensemble (compare Fig. 23 and Fig. 20). This is a new aspect of the inequivalence of statistical ensembles for self-gravitating systems.

5 Conclusion

In this paper, we have discussed the structure and the stability of self-gravitating polytropic spheres in the framework of a *generalized thermodynamics*. This framework allows us to present and organize the results in an original manner. This concept of generalized thermodynamics is rigorously justified in the case of anomalous diffusion, when the diffusion coefficient depends on the density of particles. In this paper, we have explicitly studied the nonlinear Smoluchowski-Poisson system corresponding to a power-law dependence of the diffusion coefficient. This particular situation is connected to Tsallis generalized thermodynamics [18] but more general Fokker-Planck equations can be constructed and studied [16]. Our results can also be used to study the nonlinear dynamical stability of stellar polytropes (with respect to the Vlasov-Poisson system), gaseous polytropes (with respect to the Jeans-Euler equations) and polytropic vortices (with respect to the 2D Euler equation). Indeed, the condition of nonlinear dynamical stability can be put in a form *analogous* to a problem of generalized thermodynamics (see [20, 16]

and references therein). In our approach, what we mean by generalized thermodynamics is the extension of the usual variational principle of ordinary thermodynamics (maximization of the Boltzmann entropy S_B at fixed mass M and energy E) to a larger class of functionals (called generalized entropies) [16]. This variational problem can arise in various domains of physics (or biology, economy,...) for different reasons. It is quite relevant to develop a *thermodynamical analogy* and use a vocabulary borrowed from thermodynamics (chemical potentials, inverse temperature, caloric curves, free energies,...) even if the initial problem giving rise to this variational principle is not directly connected to thermodynamics. Thus, we can directly transpose the methods developed in the context of ordinary thermodynamics (e.g., turning point arguments, bifurcations,...) to a new context.

On a technical point of view, we have provided the complete equilibrium phase diagram of self-gravitating polytropic spheres for arbitrary value of the polytropic index n and space dimension D . Our study, generalizing the classical study of Emden [32] and Chandrasekhar [14], shows how the phase portraits previously reported in the literature (for particular dimensions and polytropic indices) connect to each other in the full parameter space. From the geometrical structure of the generalized caloric curves, we can immediately determine the domains of stability of the polytropic spheres by using the turning point method [25]. These stability results have been confirmed by explicitly evaluating the second order variations of entropy or free energy. This eigenvalue method provides, in addition, the form of the density profile that triggers the instability at the critical points. Interestingly, this study can be performed analytically or by using simple graphical constructions in the Milne plane.

Finally, we have studied in detail the nonlinear Smoluchowski-Poisson system which forms a prototypical dynamical model of self-gravitating polytropes. The connection between thermodynamical and dynamical stability for this type of generalized Fokker-Planck equations has been established in the general case in [16]. The nonlinear Smoluchowski-Poisson system can have physical applications in the context of the chemotaxis for bacterial populations. The collapse and aggregation of bacterial populations is similar, in some respect, to the phenomenon of *core collapse* in globular clusters and the neglect of inertia is rigorously justified in biology (at variance with stellar systems). In addition, biological systems are likely to experience anomalous diffusion so that the NSP system can provide an interesting and relevant model for the problem of chemotaxis. We have shown that these equations can either converge toward a complete polytrope or an incomplete polytrope restrained by the box, or lead to a situation of gravitational collapse. The determination of the scaling exponent α in the microcanonical ensemble is difficult due to the extremely slow entry of the system in the scaling regime. However, it seems to be given asymptotically by $\alpha_n = 2n/(n - 1)$ ($\alpha = 2$ for isothermal spheres) as in the canonical ensemble (constant temperature). We expect that an exponent $\alpha > \alpha_n$ will be selected when the temperature is allowed to vary in space [31].

A Virial theorem in D dimensions

We define the Virial of the gravitational force in dimension D by

$$(175) \quad \mathcal{V}_D = \int \rho \mathbf{r} \cdot \nabla \Phi d^D \mathbf{r}.$$

For a spherically symmetric system, the Gauss theorem can be written

$$(176) \quad \frac{d\Phi}{dr} = \frac{GM(r)}{r^{D-1}}, \quad M(r) = \int_0^r \rho S_D r^{D-1} dr.$$

Therefore, the Virial is equivalent to

$$(177) \quad \mathcal{V}_D = \int_0^R \frac{dM}{dr} \frac{GM(r)}{r^{D-2}} dr = \frac{G}{2} \int_0^R \frac{dM^2}{dr} \frac{1}{r^{D-2}} dr.$$

In $D = 2$, one has directly

$$(178) \quad \mathcal{V}_2 = \frac{GM^2}{2}.$$

If now $D \neq 2$, we obtain after an integration by parts

$$(179) \quad \mathcal{V}_D = \frac{GM^2}{2R^{D-2}} + \frac{1}{2}(D-2) \int_0^R \frac{GM(r)^2}{r^{D-1}} dr,$$

or, using Eq. (176)

$$(180) \quad \mathcal{V}_D = \frac{GM^2}{2R^{D-2}} + \frac{1}{2G}(D-2) \int_0^R \left(\frac{d\Phi}{dr} \right)^2 r^{D-1} dr.$$

Now, using the Poisson equation (4), the potential energy can be written

$$(181) \quad W = \frac{1}{2} \int \rho \Phi d^D \mathbf{r} = \frac{1}{2S_D G} \int \Phi \Delta \Phi d^D \mathbf{r}.$$

Integrating by parts, we obtain

$$(182) \quad W = \frac{1}{2S_D G} \left\{ \Phi(R) \frac{d\Phi}{dr}(R) S_D R^{D-1} - \int_0^R \left(\frac{d\Phi}{dr} \right)^2 r^{D-1} S_D dr \right\}.$$

The gravitational potential at the exterior of the box is

$$(183) \quad \frac{d\Phi}{dr} = \frac{GM}{r^{D-1}}, \quad \Phi = -\frac{GM}{(D-2)r^{D-2}}, \quad r \geq R.$$

Introducing these results in Eq. (182) and comparing with Eq. (180), we obtain

$$(184) \quad \mathcal{V}_D = -(D-2)W, \quad D \neq 2.$$

By using the Virial tensor method introduced by Chandrasekhar, see Ref. [24], we can show that the foregoing relation remains valid if the system is not spherically symmetric.

If now the system is in hydrostatic equilibrium, we have

$$(185) \quad \nabla p = -\rho \nabla \Phi.$$

Inserting this relation in the Virial (175) and integrating by parts, we get

$$(186) \quad \mathcal{V}_D = - \oint p \mathbf{r} \cdot d\mathbf{S} + 2K,$$

where we have used $K = (D/2) \int p d^D \mathbf{r}$. This is the expression of the Virial theorem in its general form. Assuming now that p_b is uniform on the domain boundary (which is true at least for a spherically symmetric system), we have

$$(187) \quad \oint p \mathbf{r} \cdot d\mathbf{S} = p_b \oint \mathbf{r} \cdot d\mathbf{S} = p_b \int \nabla \cdot \mathbf{r} d^D \mathbf{r} = p_b D V_D R^D.$$

Therefore, for a spherically symmetric system, the Virial theorem reads

$$(188) \quad 2K - \mathcal{V}_D = p(R) D V_D R^D,$$

where \mathcal{V}_D is given by Eqs. (178) and (184). It is interesting to consider a direct applications of the Virial theorem. In $D = 2$, the Virial theorem reads

$$(189) \quad 2K - \frac{GM^2}{2} = 2\pi R^2 p(R).$$

For an isothermal gas $K = MT$ so that

$$(190) \quad 2MT - \frac{GM^2}{2} = 2\pi R^2 p(R).$$

From this relation, we conclude that there exists an equilibrium solution with $p(R) = 0$ at $T_c = GM/4$. We therefore recover the critical temperature of an isothermal self-gravitating gas in two-dimensions (see, e.g., [3]). At $T = T_c$, the density profile is a Dirac peak so that $p(R) = 0$. For $T < T_c$, there is no static solution and the system undergoes a gravitational collapse studied in [3] with the Smoluchowski-Poisson system.

B Second order variations of generalized entropy and free energy

According to Eq. (19), the variations of entropy up to second order are

$$(191) \quad \delta S = \frac{D-2n}{2} \left(\beta \int \delta p d^D \mathbf{r} + \delta \beta \int p d^D \mathbf{r} + \int \delta \beta \delta p d^D \mathbf{r} \right).$$

On the other hand, according to the polytropic equation of state (14), we have

$$(192) \quad \delta p = \gamma \frac{\delta \rho}{\rho} p + \frac{\gamma p}{n} \frac{(\delta \rho)^2}{2\rho^2} + \frac{\delta K}{K} p + \gamma \frac{\delta K}{K} \frac{\delta \rho}{\rho} p.$$

From Eqs. (9) and (15), we have

$$(193) \quad K \sim \beta^{\frac{D-2n}{2n}},$$

so that to second order

$$(194) \quad \frac{\delta K}{K} = \frac{D-2n}{2n} \frac{\delta \beta}{\beta} + \frac{(D-2n)(D-4n)}{8n^2} \left(\frac{\delta \beta}{\beta} \right)^2.$$

Inserting Eqs. (194) and (192) in Eq. (191), we get

$$(195) \quad \delta S = \frac{D-2n}{2} \left[\beta\gamma \int \frac{\delta\rho}{\rho} p d^D \mathbf{r} + \frac{\beta\gamma}{2n} \int \frac{p}{\rho^2} (\delta\rho)^2 d^D \mathbf{r} + \frac{D}{2n} \int p \delta\beta d^D \mathbf{r} \right. \\ \left. + \frac{\gamma D}{2n} \delta\beta \int \frac{\delta\rho}{\rho} p d^D \mathbf{r} + \frac{D(D-2n)}{8n^2} \frac{(\delta\beta)^2}{\beta} \int p d^D \mathbf{r} \right].$$

Now, the conservation of energy (18) implies that

$$(196) \quad 0 = \delta E = \frac{D}{2} \int \delta p d^D \mathbf{r} + \frac{1}{2} \int \delta\rho \delta\Phi d^D \mathbf{r} + \int \Phi \delta\rho d^D \mathbf{r}.$$

Inserting Eqs. (192) and (194) in Eq. (196), we obtain

$$(197) \quad \frac{D-2n}{2} \left[\frac{\gamma D}{D-2n} \beta \int \frac{\delta\rho}{\rho} p d^D \mathbf{r} + \frac{\gamma D}{2n(D-2n)} \beta \int p \frac{(\delta\rho)^2}{\rho^2} d^D \mathbf{r} + \frac{D}{2n} \int \delta\beta p d^D \mathbf{r} \right. \\ \left. + \frac{D(D-4n)}{8n^2} \frac{(\delta\beta)^2}{\beta} \int p d^D \mathbf{r} + \frac{\gamma D}{2n} \delta\beta \int \frac{\delta\rho}{\rho} p d^D \mathbf{r} \right] \\ + \frac{1}{2} \beta \int \delta\rho \delta\Phi d^D \mathbf{r} + \beta \int \Phi \delta\rho d^D \mathbf{r} = 0.$$

Subtracting this relation from Eq. (195), we get

$$(198) \quad \delta S = -\beta\gamma n \int \frac{\delta\rho}{\rho} p d^D \mathbf{r} - \frac{1}{2} \beta\gamma \int p \frac{(\delta\rho)^2}{\rho^2} d^D \mathbf{r} + \frac{D(D-2n)}{8n} \frac{(\delta\beta)^2}{\beta} \int p d^D \mathbf{r} \\ - \frac{1}{2} \beta \int \delta\rho \delta\Phi d^D \mathbf{r} - \beta \int \Phi \delta\rho d^D \mathbf{r}.$$

Now, to first order, Eq. (197) yields

$$(199) \quad \frac{\delta\beta}{\beta} = -\frac{4n}{D(D-2n)} \frac{\int \Phi \delta\rho d^D \mathbf{r} + \frac{D}{2} \gamma \int \frac{\delta\rho}{\rho} p d^D \mathbf{r}}{\int p d^D \mathbf{r}}.$$

Substituting this relation in Eq. (198), we find that the second order variations of entropy are given by Eq. (111). To compute the second order variations of free energy $J = S - \beta E$, we can use Eqs. (195) and (196) with $\delta\beta = 0$. This yields Eq. (97).

C Some useful identities

In this Appendix, we establish the identities (121)-(123) that are needed in the stability analysis of Sec. 2.6. Using an integration by parts, we have

$$(200) \quad \int_0^\alpha \theta' \xi^D \theta^n d\xi = \int_0^\alpha \xi^D \frac{d}{d\xi} \left(\frac{\theta^{n+1}}{n+1} \right) d\xi = \frac{1}{n+1} \alpha^D \theta^{n+1}(\alpha) - \frac{D}{n+1} \int_0^\alpha \xi^{D-1} \theta^{n+1} d\xi.$$

Using the Lane-Emden equation (25) and integrating by parts, we obtain

$$(201) \quad \int_0^\alpha \theta^{n+1} \xi^{D-1} d\xi = -\alpha^{D-1} \theta(\alpha) \theta'(\alpha) + \int_0^\alpha (\theta')^2 \xi^{D-1} d\xi.$$

Using the relation

$$(202) \quad \int_0^\alpha \frac{\xi^{\frac{1+D}{2}} \theta'}{\xi} \frac{d}{d\xi} \left(\xi^{\frac{1+D}{2}} \theta' \right) d\xi = \alpha^D \theta'(\alpha)^2 - \int_0^\alpha \frac{\xi^{\frac{1+D}{2}} \theta'}{\xi} \frac{d}{d\xi} \left(\xi^{\frac{1+D}{2}} \theta' \right) d\xi + \int_0^\alpha \xi^{D-1} (\theta')^2 d\xi,$$

which results from a simple integration by parts, we get

$$(203) \quad \int_0^\alpha \xi^{D-1}(\theta')^2 d\xi = -\alpha^D \theta'(\alpha)^2 + 2 \int_0^\alpha \xi^{\frac{D-1}{2}} \frac{d}{d\xi} \left(\xi^{\frac{1+D}{2}} \theta' \right) \theta' d\xi,$$

or, equivalently,

$$(204) \quad D \int_0^\alpha \xi^{D-1}(\theta')^2 d\xi = \alpha^D \theta'(\alpha)^2 - 2 \int_0^\alpha \xi^D \theta'' \theta' d\xi.$$

Using the Lane-Emden equation (25), we find that

$$(205) \quad (D-2) \int_0^\alpha \xi^{D-1}(\theta')^2 d\xi = -\alpha^D \theta'(\alpha)^2 - 2 \int_0^\alpha \xi^D \theta' \theta^n d\xi.$$

We have three equations (200), (201) and (205) for three unknown integrals. Solving this system of algebraic equations and introducing the Milne variables (49), we obtain the identities (121)-(123).

References

- [1] P.H. Chavanis, J. Sommeria and R. Robert, *Astrophys. J.* **471**, 385 (1996).
- [2] P.H. Chavanis, C. Rosier and C. Sire, *Phys. Rev. E*, **66**, 6105 (2002).
- [3] C. Sire and P.H. Chavanis, *Phys. Rev. E*, **66**, 6133 (2002).
- [4] M.A. Herrero, E. Medina, J.J.L. Velazquez, *J. Comput. Appl. Math.*, **97**, 99 (1998).
- [5] P. Biler, G. Karch, J. Dolbeault and M.J. Esteban, *Adv. Diff. Eqs.*, **6**, 461 (2001).
- [6] C. Rosier, *C.R. Acad. Sci., Ser. I: Math.*, **332**, 903 (2001).
- [7] P. Biler and T. Nadzieja, preprint.
- [8] I.A. Guerra, M.A. Peletier and J. Williams, preprint.
- [9] H. Risken, *The Fokker-Planck equation* (Springer, 1989).
- [10] J.D. Murray, *Mathematical Biology* (Springer, 1991).
- [11] P.H. Chavanis, *Phys. Rev. E* **58**, R1199 (1998).
- [12] P.H. Chavanis, *Phys. Rev. E* **64**, 6309 (2001).
- [13] P.H. Chavanis in *Dynamics and Thermodynamics of Systems with Long Range Interactions*, edited by T. Dauxois, S. Ruffo, E. Arimondo, M. Wilkens, (Lecture Notes in Physics Vol. 602, Springer 2002). e-print [cond-mat/0212223]
- [14] S. Chandrasekhar, *An introduction to the theory of stellar structure* (Dover, 1939).
- [15] C. Sire and P.H. Chavanis, in preparation.
- [16] P.H. Chavanis, submitted to *Phys. Rev. E* [cond-mat/0209096].
- [17] M. Shiino, preprint.
- [18] C. Tsallis, *J. Stat. Phys.* **52**, 479 (1988)
- [19] C. Tsallis and D.J. Bukman, *Phys. Rev. E* **54**, R2197 (1996)
- [20] P.H. Chavanis, *Astron. Astrophys.* in press [astro-ph/0207080].
- [21] A. Taruya and M. Sakagami, *Physica A* **307**, 185 (2002).
- [22] A. Taruya and M. Sakagami, *Physica A*, in press [cond-mat/0204315] .
- [23] P.H. Chavanis, *Astron. Astrophys.* **386**, 732 (2002).
- [24] J. Binney and S. Tremaine, *Galactic Dynamics* (Princeton Series in Astrophysics, 1987).
- [25] J. Katz, *Mon. Not. R. astr. Soc.* **183**, 765 (1978).
- [26] T. Padmanabhan, *Phys. Rep.* **188**, 285 (1990).
- [27] P.H. Chavanis, *Astron. Astrophys.* **356**, 1089 (2000).

- [28] D. Lynden-Bell and R. Wood, Mon. Not. R. astr. Soc. **138**, 495 (1968).
- [29] H. Cohn, Astrophys. J. **242**, 765 (1980).
- [30] D. Lynden-Bell and P.P. Eggleton, Mon. Not. R. astr. Soc. **191**, 483 (1980).
- [31] C. Sire and P.H. Chavanis, in preparation.
- [32] R. Emden, *Gaskugeln* (Teubner Verlag, Leipzig, 1907).